7.

MAGNETIC METHODS APPLIED TO BASE METAL EXPLORATION

Peter J. Hood, M.T. Holroyd, and **P.H. McGrath**
Geological Survey of Canada

Hood, Peter J., Holroyd, M.T., and McGrath, P.H., Magnetic methods applied to base metal exploration; in Geophysics and Geochemistry in the Search for Metallic Ores; Peter J. Hood, editor; Geological Survey of Canada, Economic Geology Report 31, p. 77-104, 1979.

Abstract

During the past decade, both ground and airborne magnetometers have been improved considerably by miniaturization and made more reliable by the extensive use of integrated circuit devices. For aeromagnetic surveys, proton precession magnetometers are now in common use for standard-sensitivity surveys in inboard installations and their sensitivity is commonly 1.0 gammas or better. An inboard vertical gradiometer has been fabricated by the Geological Survey of Canada using single-cell optical absorption magnetometers; results from test surveys clearly demonstrate the superior resolution of the gradiometer compared to total field results, although the line spacing for such surveys must consequently be somewhat closer. Presently a new generation of magnetometer is under active development which utilizes superconducting quantum interference detectors (Squid). If successful, this development will result in a short-base three-component gradiometer system with a much higher sensitivity than is possible with optical-absorption magnetometers.

Digital recording of aeromagnetic survey data is now standard procedure and except for the flight path recovery process, the compilation of aeromagnetic maps is now a completely automated process. Computer contouring is more objective than hand contouring, and far less costly. Furthermore, the aesthetics of machine-produced contour maps are now almost as good as the manual product. The grid data generated for the machine contouring process also facilitate the production, efficiently and at low cost, of a variety of derived and processed maps, to any scale or map projection for use in the subsequent interpretation of the aeromagnetic data.

Quantitative interpretation methods of magnetic survey data have also been improved considerably over the past decade. Several automated techniques for aeromagnetic profile data have been introduced which produce continuous depth-to-causative body profiles although the results of such routine procedures must be modified by the interpreter to take account of strike direction and the finite lengths of the causative bodies. Several three-dimensional "best-fit" interpretation techniques for individual anomalies have been published in recent years which are quite general with regard to the geometry and magnetization vector of the causative body. These techniques may also be programmed so that the results may be viewed on an interactive graphics terminal so that the interpreter can constrain various parameters to conform to the known geological realities.

Résumé

Au cours de la dernière décennie, on a amélioré de façon considérable, grâce à la miniaturisation, les magnétomètres aéroportés et terrestres; de même, on les a rendu plus fiables grâce à l'utilisation poussée de dispositifs à circuit intégré. En ce qui concerne les levés aéromagnétiques, les magnétomètres à protons sont maintenant d'utilisation courante pour les levés à sensibilité normale à bord des avions et leur niveau de sensibilité est habituellement de 1,0 gamma ou d'un niveau meilleur. Un gradiomètre vertical embarqué a été construit par la Commission géologique du Canada: il utilise des magnétomètres à absorption optique à cellule simple. Les résultats des levés démontrent clairement que le gradiomètre a une résolution supérieure à l'ensemble des résultats sur le terrain, quoique l'espacement linéaire des levés soit nécessairement un peu plus serré. A l'heure actuelle, on est à mettre au point une nouvelle génération de magnétomètres utilisant des détecteurs superconducteurs à interférence quantique (Squid). S'ils s'avèrent un succès, il en résultera un système à base courte de gradiomètres à trois éléments, d'une sensibilité plus élevée qu'il est possible d'atteindre avec les magnétomètres à absorption optique.

L'enregistrement numérique des données aéromagnétiques est maintenant chose courante, à l'exception du procédé de correction de la trajectoire de vol, l'établissement des cartes aéromagnétiques est entièrement automatisé. Le traçage des courbes par ordinateur est plus objectif que le traçage à la main, et de loin plus économique. Bien plus, la présentation des cartes en courbes produites mécaniquement est maintenant presque aussi bonne que celle des cartes produites à la main. Les données de quadrillage fournies par le procédé mécanique de traçage des courbes facilitent également la production, de façon plus efficace et à un coût moindre, d'une gamme de cartes dérivées et traitées, à n'importe quelle échelle ou projection cartographique devant être utilisées lors de l'interprétation ultérieure des données aéromagnétiques.

Les méthodes d'interprétation quantitative des données magnétiques ont aussi été considérablement améliorées au cours de la dernière décennie. Plusieurs techniques automatisées de profilage aéromagnétique ont été introduites; elles permettent de produire des profils continus de profondeur des masses, bien que les résultats de tels procédés de routine doivent être modifiés par l'interprète afin de tenir compte de la direction de trace horizontale et des longueurs limites des masses. Plusieurs techniques tridimensionnelles d'interprétation "idéales" d'anomalies individuelles ont été publiées au cours des dernières années; elles sont quelque peu générales du point de vue de la géométrie et du vecteur de magnétisation de la masse. Ces techniques peuvent également être programmées de façon à ce que les résultats puissent être visionnés sur un terminal de dialogue des graphiques; l'interprète peut ainsi rendre certains paramètres conformes aux réalités géologiques connues.

INTRODUCTION

More than 500 articles dealing with the magnetic survey technique have been published since the first symposium in 1967 so it is possible to give more than a condensed overview of the significant progress that has been made in the past decade in this review; we will, therefore, present what appear to us to be the highlights with a consequent but unavoidable omission of much important work.

There have been some important reviews published in the last decade. A comprehensive review of aeromagnetic survey instrumentation and techniques was published by Hood and Ward (1969). For general reviews of data processing and interpretation, the reader is referred to the articles by Steenland (1970) and by Grant (1972).

Units Used in Magnetic Surveying

In September 1973, the International Association of Geomagnetism and Aeronomy recommended the adoption of Systeme International (SI) units in the field of geomagnetism. Of main interest to exploration geophysicists are the SI units for magnetic field (T), intensity of magnetization (J) and volume susceptibility (k) and the changes are briefly reviewed in the following discussion. For further elaboration the reader is referred to Hahn (1978) and to IAGA (1973); an understanding of the units used in geomagnetism appears to have been somewhat obfuscated by the adoption of SI units, and what follows, therefore, is mainly intended for the guidance of exploration geophysicists.

Magnetic Field (T)

In practice, the SI and cgs units of magnetic field are the tesla and oersted respectively and their relationship is

$$1 \text{ tesla} = 10\,000 \text{ oersteds}$$

which is, however, a rather large unit for magnetic survey use. The unit in common usage by exploration geophysicists for at least 50 years is the gamma (symbol γ) and

$$1 \text{ gamma} = 10^{-5} \text{ oersted}$$

so that 1 gamma $= 10^{-9}$ teslas $= 1$ nanotesla (symbol nT)

$$= \frac{10^{-2}}{4\pi} \text{ Am}^{-1} \simeq 8 \times 10^{-4} \text{ Am}^{-1}$$

In the IAGA resolution adopted at the 1973 meeting in Kyoto, Japan, it was perhaps anticipated that common usage would keep the gamma alive for the following statement was made: "If it is desired to express values in gammas, a note should be added stating that 'one gamma is equal to one nanotesla'".

Intensity of Magnetization (J)

In the cgs system, the units of magnetization were usually expressed in emu units. In SI, the units are ampere per metre and the relationship is 1 emu = 10^3Am^{-1} so that

$$J_{emu} \times 10^{-6} \text{ emu} = J_{SI} \times 10^{-3} \text{ Am}^{-1} = J_{SI} \text{mAm}^{-1}$$

i.e. milliamp per metre.

Susceptibility (k)

Volume susceptibility was usually expressed in dimensionless cgs units as $\times 10^{-6}$ emu/cc or cgsu. For SI units, 1 cgsu of susceptibility = $1/4\pi$ SI unit of susceptibility, i.e.

$$k_{SI} = 4\pi k_{cgs}$$

and common usage is to express volume susceptibility in $\times 10^{-3}$ SI units so that 1000×10^{-6} emu/cc = 12.6×10^{-3} SI units.

Because volume susceptibility is the ratio between the induced intensity of magnetization and applied magnetic field which are both expressed in Am^{-1}, it results in the necessity of expressing susceptibility in the somewhat meaningless terms of SI units. Actually susceptibility (or rather permeability) is a fundamental physical constant and should therefore have its own units. Accordingly for exploration geophysicists it would be convenient if the $\times 10^{-3}$ SI susceptibility unit were called a kappa; then for the induced magnetization case

$$k_{SI} = \frac{J_{SI} \text{ in mAm}^{-1}}{T \text{ in gammas}} \times \frac{4\pi}{10}$$

so that k_{SI} in kappas $= \dfrac{J_{SI} \text{ in mAm}^{-1}}{T \text{ in gammas}} \times 400\pi$

Thus, a rock with 1 per cent magnetite by volume which usually has a susceptibility of about 3000×10^{-6} emu/cc, would have a susceptibility of 37.7 kappas, which is a convenient size number to deal with.

MAGNETIC SURVEY INSTRUMENTATION

During the past decade, both ground and airborne magnetometers have been improved considerably by miniaturization and made more reliable by the extensive utilization of integrated circuit devices. The theory of operation of the various types of magnetometer and much additional background material was published in the proceedings volume for the 1967 symposium held in Niagara Falls (Hood, 1970) and will not be repeated here.

Ground Survey Magnetometers

For ground magnetometers, the mechanical balance type has been almost completely replaced in survey use throughout the world by electronic magnetometers because of the higher rate of survey production that can be achieved with the latter and the fact that electronic magnetometers have a higher sensitivity. There are two main types of ground magnetometer in common survey use for mineral exploration, namely the fluxgate and proton free-precession magnetometer (Table 7.1).

Ground Fluxgate Magnetometers

The typical fluxgate magnetometer weighs from 1.5 to 4 kg (that is 3 to 9 lb), measures the vertical component of the earth's magnetic field and in survey use is carried by a strap worn around the operator's neck (see Fig. 7.1). The range of a typical fluxgate instrument is $\pm 100\,000\ \gamma$ which is more than adequate for worldwide use except over very strongly magnetized iron formation. The majority of ground fluxgate magnetometers have a meter as the readout device with the highest sensitivity selectable usually being 10 or 20 γ per small division. However, Scintrex manufacture a one-gamma digital fluxgate magnetometer, the MFD-4, in which the vertical component is read from a five-digit light-emitting diode display.

In 1977, Littlemore Scientific Engineering of Oxford, U.K. produced a fluxgate gradiometer which has a differential resolution of 0.5 γ. The 4.6 kg Elsec 781 fluxgate gradiometer (Fig. 7.2) consists of two fluxgate elements mounted coaxially 1 m apart at the ends of a Pyrex glass tube which has a low coefficient of thermal expansion and therefore negligible temperature effect. Thus the instrument measures the vertical gradient of the vertical component of the earth's magnetic field with a resolution of 0.5 γ/m. The

Table 7.1

Commercially available electronic magnetometers for ground prospecting. All magnetometers are hand held and operate from rechargeable batteries or cells (from Hood, 1978)

Type	Manu-facturer	Model designation	Component measured T or V	Readout display	Sens in gammas	Range in gammas (K=1000)	Weight in field use	Power Source
Fluxgate	Adams Marine (Canada)	Sable Mark 2	V	Meter	20q/div	100K	4 kg	9 VDC transistor cell
	Littlemore (UK)	Elsec 781	V & vert. grad.	LCD Bar	0.5γ	± 5000q/m	kg	18 V Pb-acid battery
	McPhar (Canada)	M700	V	Meter	20q/div	±100K	3.8 kg	18 VDC 9V or C cells
	Phoenix (Canada	MV-1	V	Meter	20q/div	±100K	1.7 kg	2x6 V gel-cell batteries
	Scintrex (Canada)	MF2-100 MFD-4	V V	Meter 5 digit LED	2q/div 1	±200K ± 99 999	2.9 kg 2.1 kg	24 VDC cells 4 D cells or 6V Pb-acid battery
Proton precession	Austral (Australia)	PPM-1	T	5 digit	1γ	20 to 100K	6.8 kg	12-15 VDC D cells or Pb acid battery
	Barringer (Canada	GM-122	T	5 digit LED	1γ	20 to 100K	5.1 kg	18 VDC 12 D cells
	Geometrics (US)	G816	T	5 digit	1γ	20 to 100K	2.8 kg	18 VDC D cells
		G836	T	4 digit	10γ		2 kg	12 VDC
	Littlemore (UK)	Elsec 595	T	5 digit Nixie	1γ	24 to 72K	6.7 kg	17 VDC Nicad battery
		Elsec 770	T	LCD	0.25γ	20 to 90K	2.5 kg	18 VDC D cells
	Scintrex (Canada)	MP-4	T	5 digit LED	1γ	20 to 100K	3.7 kg	12 VDC 8 D cells
Optical absorption	Varian (Canada)	VIW 2302	T & gradient	LED Audio	0.1q and 0.1γ/m	20 to 100K	12.5 kg	30 VDC 5 gel-cell batteries

electronic circuitry utilizes Cmos components and a novel readout method. The output of the differential fluxgates is in analog form which can be used for any external recorder system; the output signal is digitized and displayed on a liquid-crystal two-level bar readout. The bar readout combines the analog aspect of travelling in a positive or negative direction but at the same time giving a precise digital indication. Two parallel bar displays are provided, one having 10 times the resolution of the other. Besides this visual readout, an audio signal is provided when the field change exceeds a front panel preset value. The Elsec 781 fluxgate gradiometer is intended for archeological investigations and should be of particular value in the search for ferrous objects, e.g. steel pipes, munitions, located some distance below the ground which are beyond the limited range of mine detector-type devices.

Ground Proton Precession Magnetometers

Ground proton precession magnetometers have been improved considerably over the past decade particularly with respect to their weight in field use, their ability to function properly in high magnetic field gradients and lower power consumption. A typical ground proton precession magnetometer measures the total intensity of the earth's magnetic field which is read on a LED display with a sensitivity of one gamma or better, weighs from 2.5 to 7 kg (5 to 15 lb) and operates over the range 20 000 to 100 000 γ using Nicad or lead-acid batteries. Figure 7.3 shows the Scintrex MP-4 instrument which uses an optimized noise-cancelling dual sensor with a gradient tolerance of 5000 γ/m. An indicator light warns of excessive gradient, ambient noise or electronic failure and a digital readout of the battery voltage indicates whether the batteries should be replaced. Many of the ground proton precession magnetometers can be used without modification as diurnal base station monitors with a suitable digital or analog chart recorder.

Optical Absorption Magnetometers

In 1975, Varian Associates of Georgetown, Ontario introduced a portable cesium-vapour magnetometer, the V1W-2302, which was intended to be used to search for ferro-magnetic objects such as pipelines or in archeological investigations. In 1977, Varian introduced a gradiometer version of the same instrument which was designated the V1W-2302C1 (Fig. 7.4). The V1W-2302C1 is an instrument that uses two cesium magnetometers to determine the

Figure 7.1. *McPhar M700 fluxgate magnetometer with strap around operator's neck, being operated on the Cavendish geophysical test range, southwestern Ontario; McPhar Instrument Corp., Willowdale, Ontario. (GSC 202228-G)*

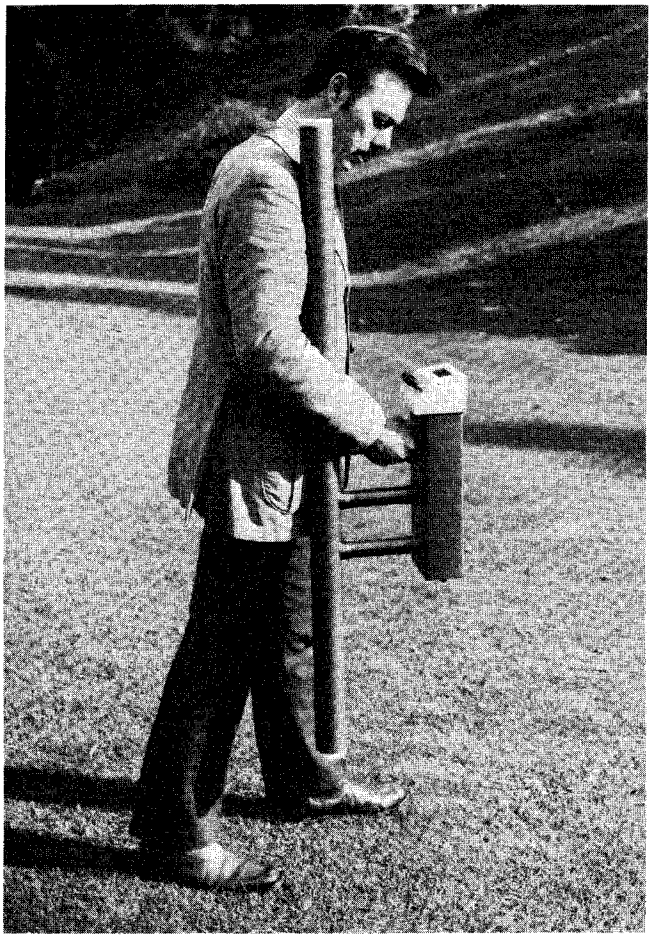

Figure 7.2. *Elsec 781 digital fluxgate gradiometer; Littlemore Scientific Engineering Co., Oxford, U.K. (GSC 203492-O)*

magnitude of the magnetic field intensity at two points spaced 2 m apart. By subtracting the two measured values, a gradient of the total field intensity can be determined. The sensitivity of the gradient measurement is ±0.1 γ/2 m and the range is ±9000 γ/2 m. The instrument is also designed to work in the so-called variometric mode whereby one Cs sensor is stationary while the other, connected via a single coaxial cable, is used as a mobile sensor. In this mode a very detailed survey of an area may be conducted with the results being independent of time-varying components of the earth's magnetic field, i.e. diurnal changes and micropulsations. Each of the two Varian cesium sensors can also be used for the total field measurements. In this mode of operation, the magnitude of the magnetic field intensity can be measured over the range of 20 000 to 100 000 γ, which permits the instrument to be used for magnetic surveys in any part of the world. The sensitivity of the measurements is ±0.1 γ and the absolute accuracy is ±0.5 γ. In all three modes of operation (gradiometer/variometer/total field magnetometer) the results are displayed in the form of a 6-digit number by a 7 segment incandescent display on the 2.1 kg console. The display is updated 2 times per second. In addition to the visual display, an audio output is available whose frequency is 7 Hz/γ in the total field mode and 7 Hz per 1 γ/2 m in the gradiometric mode. The audio display permits a rapid survey for localized magnetic anomalies due to buried artifacts. The visual display update time is limited by the human response. The instrument takes measurements at the rate of 11 times per second and each of the measurements takes 0.045 seconds. This information is available in the digital (BCD) form or analog form (potentiometric or galvanometric) for the recording version of the instrument. The Varian V1W-2302C1 portable gradiometer is powered by 5 gel rechargeable batteries connected in series (providing 30 V) for periods of up to 6 hours before the batteries have to be recharged; the temperature operating range is 0° to 50°C.

Instrumentation for Magnetic Property Measurements

It is often useful to investigate the magnetic properties of a rock formation to ascertain whether it has sufficient magnetization to produce a given anomaly or whether the direction of the magnetization vector differs markedly from that of the present earth's field e.g. is reversed. The magnetization (J) of a given rock formation is due to two components, namely the induced and the remanent magnetization (R). These are vectors and the induced magnetization is accurately aligned in the direction of the earth's magnetic field (T).

Figure 7.3. *Scintrex MP-4 direct-reading proton precession magnetometer; Scintrex Ltd., Toronto, Ontario. (GSC 202228-E)*

Figure 7.4. *V1W-2302C1 cesium gradiometer; Varian Associates, Georgetown, Ontario. (GSC 203492-T)*

Thus $\bar{J} = k\bar{T} + \bar{R}$

where k is the susceptibility of the rock formation. Thus in order to ascertain the total magnetization of a rock formation it is necessary to measure both the susceptibility and the remanent magnetization vector.

Susceptibility Meters

The preferred technique in measuring the susceptibility of a given rock formation is to carry out in situ measurements because this physical parameter is somewhat variable and a representative determination cannot normally be made from a few hand specimens.

Table 7.2 lists the susceptibility meters which are presently available. Several portable susceptibility meters have appeared in the last decade. One example is the Elliot PP-2A instrument (Fig. 7.5) which weighs 0.5 kg and may be used to measure the susceptibility of hand and drill core samples or for in situ measurements on outcropping rock formations. The direct digital readout of susceptibility to two significant figures over the range 100×10^{-6} to $99\,000 \times 10^{-6}$ cgsu (1244×10^{-3} SIu) may be obtained with a resolution of 100×10^{-6} cgsu (0.13×10^{-3} SIu) by pushing a button. The instrument may also be calibrated in percentage magnetite equivalents for the direct logging of drill core for magnetite content.

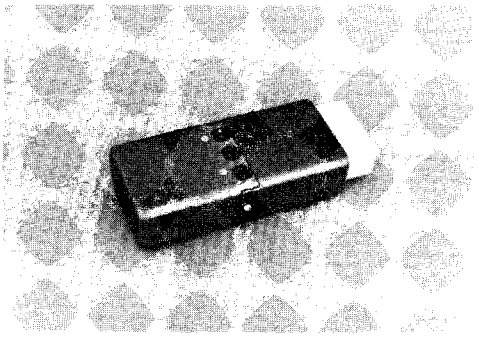

Figure 7.5. *Elliot PP-2A susceptibility meter; Elliot Geophysical Co., Tucson, Arizona. (GSC 203492-S)*

times, took only 10 minutes. The JR-2 had a sensitivity of 4 x 10^{-6} Am^{-1}. It did not require any special laboratory conditions. The LAM-1 astatic magnetometer was capable of measuring the remanence, susceptibility, and susceptibility anisotropy using irregular and large sized rock samples. The sensitivity of the LAM-1 was about 1.6 x 10^{-5} Am^{-1}, i.e. 2 x 10^{-7} Oe. In 1973, the range of LAM astatic magnetometers was increased by the introduction of three new models. The basic, simplest version LAM-2 measures the astatic system deflection by a light beam spot on a graduated scale with sensitivity 4 x 10^{-15} to 6 x 10^{-6} Am^{-1} scale division (5 x 10^{-7} to 5 x 10^{-8} Oe/scale division). The LAM-3 incorporates an electronic negative feedback loop and system deflection is displayed on an analog indicator. This gives a shorter setting time, stabilizes the sensitivity and allows simple range selection. A digital output device converts the LAM-3 to a LAM-3D which permits automatic data recording for computer handling. The LAM-4 has automatic ranging which further shortens the measuring time. The LAM-3 and LAM-4 have 7 sensitivity ranges from 8 x 10^{-4} to 8 x 10^{-1} Am^{-1} (1 x 10^{-5} to 1 x 10^{-2} Oe/fsd). Each LAM is provided with an orthogonal manipulator that will take irregular samples of up to 10 cm diameter; a microlamp for small samples is also provided so that measurements are quickly carried out.

In 1974, the Institute of Applied Geophysics in Brno, Czechoslovakia commenced delivery of a digital version of their JR series (JR-2 and the subsequent JR-3) of spinner magnetometers. The new instrument, designated UGF-JR4 has digital indication of two simultaneous components of remanent magnetic polarization and parallel BCD output for direct computer processing of measured data. Samples may be cubes 20 x 20 x 20 mm or cylinders 25.4 mm diameter by 22 mm length. Cylinders are measurable with axis vertical or horizontal. The major improvements incorporated in the JR-4 rock magnetometer include increased sensitivity, a wider measuring range, simpler measuring procedure, automatic compensation for magnetic moment of sample holder, higher accuracy, and shorter measuring time. Some of the features of the new instrument are automatic compensation for the magnetic moment of the sample holder, use of photo transistors instead of permanent magnets to obtain the reference signal, and an automatic stopping of the sample rotation at the end of integration time. The most sensitive measuring range covers 0-9.99 picoteslas with a sensitivity of 1 pT for an integration time of 100 seconds.

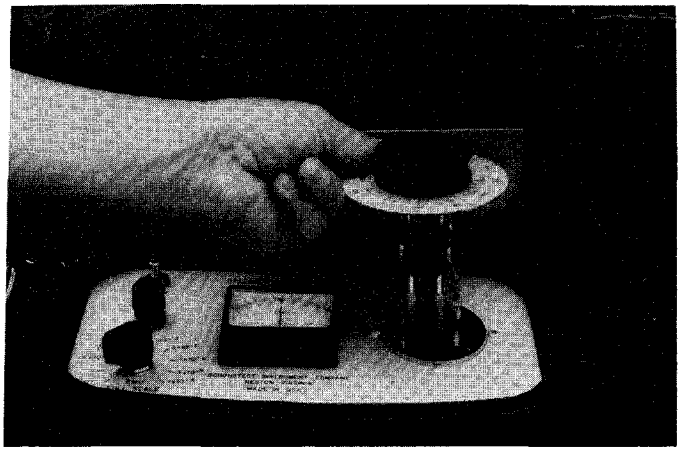

Figure 7.7. *Schonstedt PSM-1 remanent magnetometer for field measurements; Schonstedt Instrument Co., Reston, Virginia. (GSC 202228-F)*

A portable instrument designated the PSM-1 (Fig. 7.7) has been developed by Schonstedt Instrument Company of Reston, Virginia, in which the remanent magnetization of irregularly-shaped rock specimens may be measured. Full-scale ranges of 10^{-4} to 1 emu (10^{-1} to 10^{3} Am^{-1}) permit the measurement of virtually all igneous rocks and many types of sediments with an accuracy of ±10% of moment and ±5% direction angle. Schonstedt also manufactures a range of laboratory spinner magnetometers for more accurate remanent magnetism measurements.

Superconducting quantum interference device (Squid) sensors have also been developed for use in rock magnetism measurements. The interested reader is referred to an excellent review of the topic by Goree and Fuller (1976) for descriptions of the theory and design of the Squid instrumentation.

Drillhole Logging Instrumentation

For iron-ore prospecting, the measurement of the magnetic parameters of rock formations through which drillholes pass are carried out using susceptibility logging equipment or by the use of three-component fluxgate magnetometers. In 1974, Zablocki described the magnetic susceptibility system being used by the U.S. Steel Corporation at the Minntac open-pit taconite mine in northern Minnesota for short blast holes 40-60 feet (12-18 m) in depth with a diameter of 12.25 in. (31 cm). Figure 7.8 shows a schematic diagram of the system which uses an air-cored multi-turn induction coil connected to one arm of an inductance bridge and designed using an operational amplifier so that there was constant current through the induction coil. The system had a capability of measuring the Fe content in the drillholes with a standard error of ±1.2 weight per cent Fe, and was considered to be especially useful in establishing cut-off boundaries between ore and waste. In situ bulk measurements are much preferable to laboratory measurements of much smaller volumes using drill core.

In recent years much effort has been devoted in Sweden to the development of a reliable drillhole fluxgate magnetometer which would be useful for the detection of iron-ore deposits. In 1969, ABEM introduced a new version of the Swedish three-component drillhole magnetometer for EX (36 mm) holes designated the HBM 4 (Fig. 7.9). This transistorized instrument measures three orthogonal magnetic components as well as dip angle down to 1200 m (3600 ft.). The measurements have an accuracy of 50 γ within the range ±100 000 γ and 150 γ in the range ±300 000 γ. The dip of the hole is measurable from +90° (horizontal) to -40° with an accuracy of 0.5°. The major difference from the previous model is the electronic switching of fluxgate probes instead of servomotor changeover.

Lantto (1973) has presented a general interpretation procedure for magnetic logging data called the characteristic curve method. This method is based on the characteristic points of a profile where either the horizontal or vertical field components are zero. Standard curves are given in the paper for models which can be represented by two parallel infinite line poles (long tubular bodies) or dipoles (rod-shaped bodies). The standard curves were applied to determining the depth of the bottom of an iron ore deposit at the Otanmaki mine in Finland using characteristic points located on the surface and in two boreholes.

Airborne Magnetometers

Table 7.3 shows the airborne magnetometers which are commercially available at the time of writing. Direct-reading proton precession magnetometers are now in common use for standard sensitivity aeromagnetic surveys in inboard

times, took only 10 minutes. The JR-2 had a sensitivity of 4 x 10^{-6} Am^{-1}. It did not require any special laboratory conditions. The LAM-1 astatic magnetometer was capable of measuring the remanence, susceptibility, and susceptibility anisotropy using irregular and large sized rock samples. The sensitivity of the LAM-1 was about 1.6 x 10^{-5} Am^{-1}, i.e. 2 x 10^{-7} Oe. In 1973, the range of LAM astatic magnetometers was increased by the introduction of three new models. The basic, simplest version LAM-2 measures the astatic system deflection by a light beam spot on a graduated scale with sensitivity 4 x 10^{-15} to 6 x 10^{-6} Am^{-1} scale division (5 x 10^{-7} to 5 x 10^{-8} Oe/scale division). The LAM-3 incorporates an electronic negative feedback loop and system deflection is displayed on an analog indicator. This gives a shorter setting time, stabilizes the sensitivity and allows simple range selection. A digital output device converts the LAM-3 to a LAM-3D which permits automatic data recording for computer handling. The LAM-4 has automatic ranging which further shortens the measuring time. The LAM-3 and LAM-4 have 7 sensitivity ranges from 8 x 10^{-4} to 8 x 10^{-1} Am^{-1} (1 x 10^{-5} to 1 x 10^{-2} Oe/fsd). Each LAM is provided with an orthogonal manipulator that will take irregular samples of up to 10 cm diameter; a microlamp for small samples is also provided so that measurements are quickly carried out.

In 1974, the Institute of Applied Geophysics in Brno, Czechoslovakia commenced delivery of a digital version of their JR series (JR-2 and the subsequent JR-3) of spinner magnetometers. The new instrument, designated UGF-JR4 has digital indication of two simultaneous components of remanent magnetic polarization and parallel BCD output for direct computer processing of measured data. Samples may be cubes 20 x 20 x 20 mm or cylinders 25.4 mm diameter by 22 mm length. Cylinders are measurable with axis vertical or horizontal. The major improvements incorporated in the JR-4 rock magnetometer include increased sensitivity, a wider measuring range, simpler measuring procedure, automatic compensation for magnetic moment of sample holder, higher accuracy, and shorter measuring time. Some of the features of the new instrument are automatic compensation for the magnetic moment of the sample holder, use of photo transistors instead of permanent magnets to obtain the reference signal, and an automatic stopping of the sample rotation at the end of integration time. The most sensitive measuring range covers 0-9.99 picoteslas with a sensitivity of 1 pT for an integration time of 100 seconds.

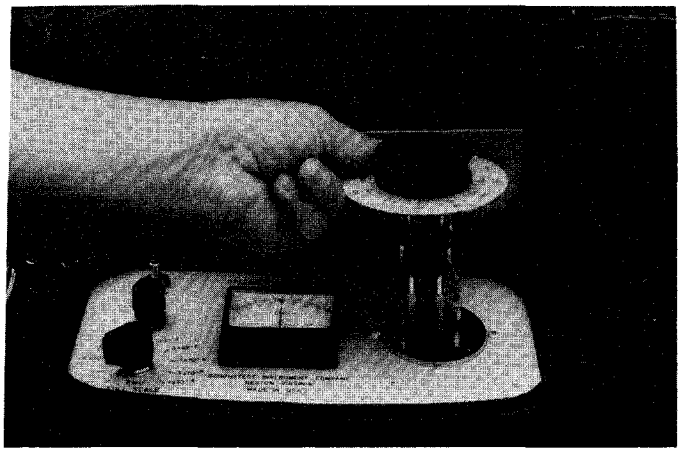

Figure 7.7. *Schonstedt PSM-1 remanent magnetometer for field measurements; Schonstedt Instrument Co., Reston, Virginia. (GSC 202228-F)*

A portable instrument designated the PSM-1 (Fig. 7.7) has been developed by Schonstedt Instrument Company of Reston, Virginia, in which the remanent magnetization of irregularly-shaped rock specimens may be measured. Full-scale ranges of 10^{-4} to 1 emu (10^{-1} to 10^{3} Am^{-1}) permit the measurement of virtually all igneous rocks and many types of sediments with an accuracy of ±10% of moment and ±5% direction angle. Schonstedt also manufactures a range of laboratory spinner magnetometers for more accurate remanent magnetism measurements.

Superconducting quantum interference device (Squid) sensors have also been developed for use in rock magnetism measurements. The interested reader is referred to an excellent review of the topic by Goree and Fuller (1976) for descriptions of the theory and design of the Squid instrumentation.

Drillhole Logging Instrumentation

For iron-ore prospecting, the measurement of the magnetic parameters of rock formations through which drillholes pass are carried out using susceptibility logging equipment or by the use of three-component fluxgate magnetometers. In 1974, Zablocki described the magnetic susceptibility system being used by the U.S. Steel Corporation at the Minntac open-pit taconite mine in northern Minnesota for short blast holes 40-60 feet (12-18 m) in depth with a diameter of 12.25 in. (31 cm). Figure 7.8 shows a schematic diagram of the system which uses an air-cored multi-turn induction coil connected to one arm of an inductance bridge and designed using an operational amplifier so that there was constant current through the induction coil. The system had a capability of measuring the Fe content in the drillholes with a standard error of ±1.2 weight per cent Fe, and was considered to be especially useful in establishing cut-off boundaries between ore and waste. In situ bulk measurements are much preferable to laboratory measurements of much smaller volumes using drill core.

In recent years much effort has been devoted in Sweden to the development of a reliable drillhole fluxgate magnetometer which would be useful for the detection of iron-ore deposits. In 1969, ABEM introduced a new version of the Swedish three-component drillhole magnetometer for EX (36 mm) holes designated the HBM 4 (Fig. 7.9). This transistorized instrument measures three orthogonal magnetic components as well as dip angle down to 1200 m (3600 ft.). The measurements have an accuracy of 50 γ within the range ±100 000 γ and 150 γ in the range ±300 000 γ. The dip of the hole is measurable from +90° (horizontal) to -40° with an accuracy of 0.5°. The major difference from the previous model is the electronic switching of fluxgate probes instead of servomotor changeover.

Lantto (1973) has presented a general interpretation procedure for magnetic logging data called the characteristic curve method. This method is based on the characteristic points of a profile where either the horizontal or vertical field components are zero. Standard curves are given in the paper for models which can be represented by two parallel infinite line poles (long tubular bodies) or dipoles (rod-shaped bodies). The standard curves were applied to determining the depth of the bottom of an iron ore deposit at the Otanmaki mine in Finland using characteristic points located on the surface and in two boreholes.

Airborne Magnetometers

Table 7.3 shows the airborne magnetometers which are commercially available at the time of writing. Direct-reading proton precession magnetometers are now in common use for standard sensitivity aeromagnetic surveys in inboard

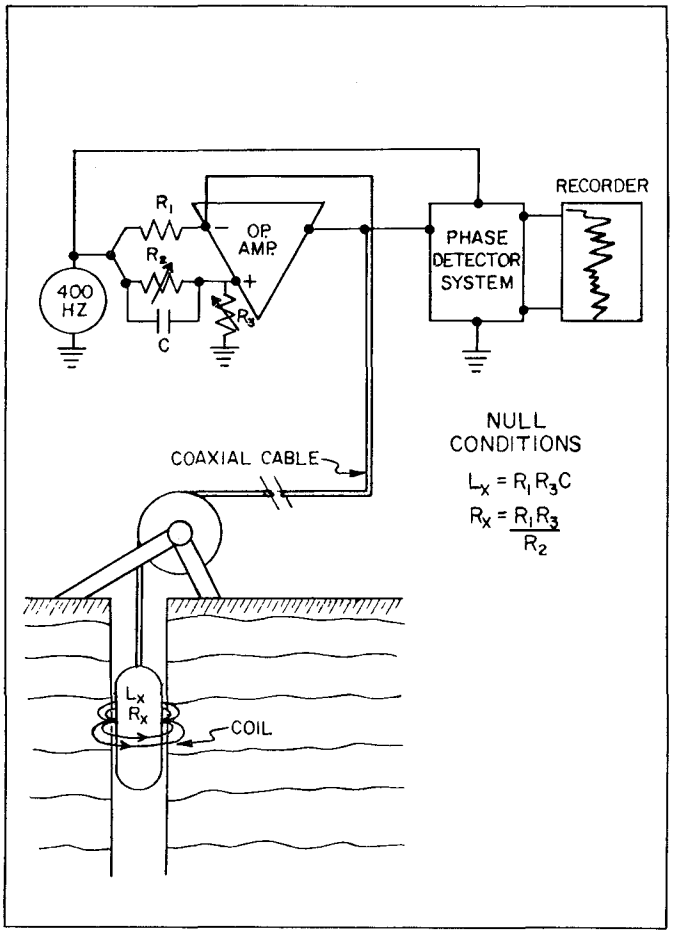

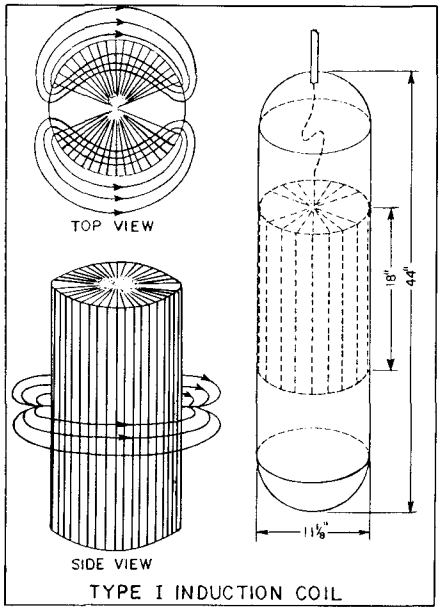

Figure 7.8. *Magnetic susceptibility drillhole logging system (Zablocki, 1974).*

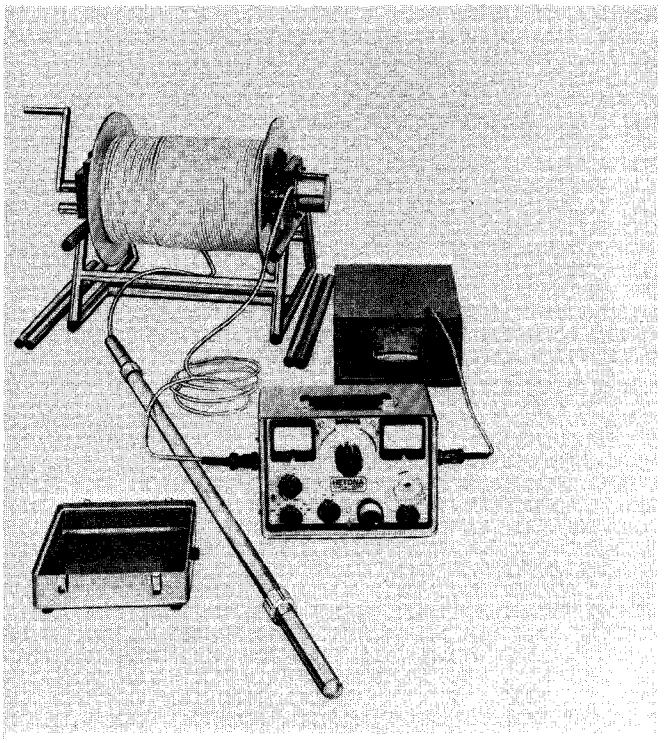

Figure 7.9. *ABEM three-component fluxgate magnetometer for drillhole logging; Atlas Copco ABEM AB, Stockholm, Sweden. (GSC 203492-U)*

installations and their sensitivity is mostly 1.0 gamma or better. However, the use of fluxgate magnetometers persists perhaps because they produce a continuous analog output instead of a stepped one and this is preferred by many magnetic interpreters who use graphical interpretation techniques. The range of airborne proton precession magnetometers is typically 20 000 to 100 000 γ and this permits their use worldwide except over the most strongly magnetized iron formations.

During 1969, Geometrics introduced their Model G-803 direct-reading airborne proton precession magnetometer (Fig. 7.10). The complete 22.3 kg aeromagnetic survey system consists of a 6.4 kg magnetometer console in a standard 19 inch rack, a 5.5 kg 13 cm chart recorder, and a bird and towing-system weighing 10.5 kg. The range of the instrument is 20 000 to 100 000 γ in 10 manually-selected overlapping ranges. The sensitivity of the standard instrument is 1 γ at a sampling rate of 1 second controlled either by external or internal automatic triggers or manually. Other options are available such as a 0.5 γ magnetometer with an 0.8 second sampling rate. The total field output of the instrument may be recorded digitally and/or potentiometrically or galvanometric analog recording employed.

Gam Service Ltd. of Grenoble, France, which is part of the French Atomic Energy Commission, is manufacturing an Overhauser proton precession magnetometer, the MPPE101, which has a 0.01 γ sensitivity at a 1 second sampling interval. The range of the 27 kg magnetometer is 20 000 to 80 000 γ. Both analog and BCD digital outputs are provided. The instrument has been used for aeromagnetic surveys and as a differential magnetometer for archeological investigations (Collin et al., 1973); it is readily apparent that it would be well suited for use in a vertical gradiometer aeromagnetic survey system.

Table 7.3

Airborne magnetometers available for purchase. All magnetometers measure the total intensity of the earth's magnetic field, have visual displays, and are direct reading

Magnet-ometer and type	Manu-facturer	Model No.	Max sens in gammas	Range in gammas (K=1000)	Sampling rate for maximum sensitivity	Readout A=Analog D=Digital	Power Require-ments	Weight (kg)
Proton precession-direct reading	Barringer (Canada)	AM 123	1γ	20-100K	1 sec	A & D	12-30VDC 5A polarize	9.1 (incl. chart recorder)
	Geometrics (US)	G 803	1γ	20-100K	1 sec	A & D	22-32VDC 150W average	6.4
	Littlemore (UK)	Elsec 5951	1γ	24-72K	1.2 sec	A & D	20-28VDC	25
		Elsec 7702	1γ	20-90K	2 sec	A	20-28VDC	7
	Sander (Canada)	NPM-5	0.1γ	20-100K	1 sec	A & D	28VDC 1A + 7A polarize	5 (console)
	Scintrex (Canada)	MAP-4	1γ	20-100K	0.5 sec	A & D	24-30VDC 3.5A max.	6 (console) 3 (sensor)
	Sonotek (Canada)	IGSS/SDS systems	0.1γ	15-100K	1 sec	A & D	28VDC	
	Varian (Canada	V-85	0.1γ	20-100K	1 sec	A & D	28VDC 4A polarize	7.7
Overhauser	Gam Service (France)	MPPE101	0.01γ	20-80K		A & D	12&28VDC 2.5A	27

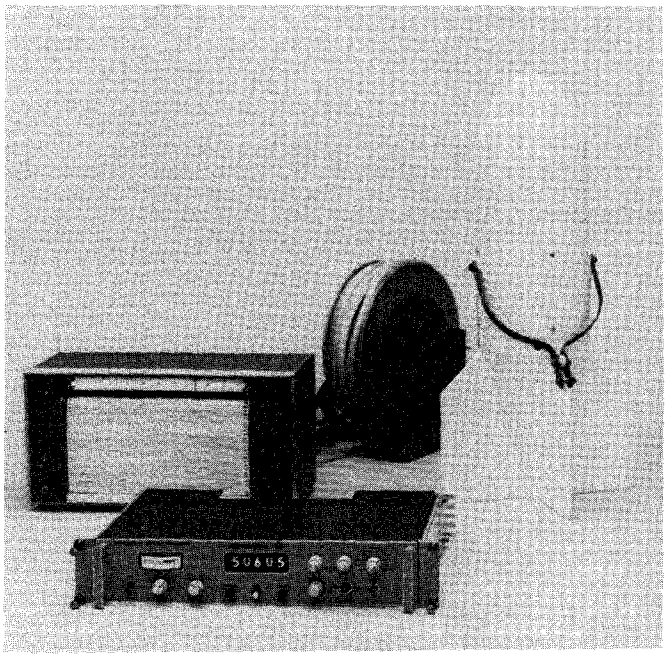

Figure 7.10. *Geometrics G803 proton precession airborne magnetometer; Geometrics Inc., Sunnydale, California (GSC 203492-R)*

Aeromagnetic Gradiometers

The use of optical absorption magnetometers for aeromagnetic surveying appears to have been mostly confined to petroleum exploration with the exception of the experimental airborne system installed inboard on a Beechcraft B80 aircraft of the Geological Survey of Canada. During the middle 70's the system was modified by the addition of a second boom (Fig. 7.11) so that the vertical gradient of the earth's total field could be measured directly (Sawatzky and Hood, 1975). The successful development of this system was only made possible by the use of two active magnetic compensation systems which are manufactured by Canadian Aviation Electronics of Montreal. The vertical separation of the single-cell self-orienting optical absorption magnetometers in the two booms is approximately 2 metres and the system is designed for gradiometer surveys of Precambrian Shield areas rather than for petroleum exploration.

With regard to the desirable sensitivity for magnetometers to be used in an inboard vertical gradiometer system, two main factors enter into the consideration: 1) the basic sensitivity of the magnetometers themselves, and 2) their vertical separation. It is clear from the results of the surveys flown at 500 feet (152 m) over the Canadian Precambrian Shield by the Geological Survey of Canada that a contour interval of at least 0.025 γ/m should be utilized in delineating magnetic gradient anomalies. Anomalies of this amplitude commonly extend across several flight lines (see Fig. 2 in Coope, 1979, where the spacing of the N-S flight lines is 1000 ft. (305 m)) and therefore reflect the presence of underlying geological features having a low magnetization contrast with respect to the surrounding rocks. The ratio between the basic sensitivity of the survey magnetometer and

Figure 7.11. *Vertical gradiometer system installed on the Beechcraft B80 Queenair aircraft of the Geological Survey of Canada. (GSC 202036-K)*

the contour interval used in the compilation of the resultant aeromagnetic maps is usually between 5:1 and 10:1 depending upon the quality of the recorded data which is affected by various factors such as the compensation figure-of-merit of the survey aircraft. For instance, using a well-compensated one-gamma magnetometer, it is quite feasible to compile the final aeromagnetic maps using a 5-gamma contour interval. Consequently an effective (Precambrian Shield) gradiometer would have to have a sensitivity of 0.005 γ/m if the resultant maps were to be compiled using a 0.025 γ/m interval. For light twin-engine aircraft which are now commonly utilized for aeromagnetic surveys, a sensor separation around 2 m is feasible for an inboard gradiometer system. In the case of the GSC Queenair B80 gradiometer (Fig. 7.11), the sensor separation is actually 2.06 m. Thus magnetometers with a minimum sensitivity of 0.01 γ are required for an inboard vertical gradiometer system to be used in aeromagnetic surveys of Precambrian terrane.

Squid Magnetometers

For total field magnetometers, the useful sensitivity that can be utilized in airborne surveys is about 0.01 γ and there would not be much point in developing more sensitive magnetometers than now exist except as gradiometers. Thus for some years now a new generation of more sensitive cryogenic gradiometer has been under active development which utilizes the Josephson junction effect; the device is usually referred to as a Squid which stands for superconducting quantum interference device. In 1969, an aeromagnetic gradiometer was developed in the Laboratory of Electronics of the University of Oulu in Finland (Otala, 1969), which had a gradient resolution of 8×10^{-3} γ/m but the project appears to be dormant at the present time. In Canada, CTF Systems Ltd. of North Burnaby, British Columbia are presently (1978) developing a six-component gradiometer system for airborne use which will permit gradient measurements in three orthogonal directions. The potential advantage of such Squid devices is that they possess a sufficiently high sensitivity that the gradient can be measured over a distance of 25 cm or less so that a gradiometer sensor can be installed in a single aircraft stinger with a realizable sensitivity of 10^{-5} gammas per metre. Sarwinski (1977) has described some of the practical considerations in the design of a Squid gradiometer.

Figure 7.12 shows a block diagram of a typical RF-driven Squid magnetometer (Goree and Fuller, 1976). The sensor is in a cryogenic environment, namely liquid helium at a temperature of 4.2°K. The superconducting drive coil is resonated close to 30 MHz by using a fixed capacitor near the sensor. The coil is connected to an RF amplifier and detector, to the audiomodulator, and to the feedback circuit. The sensor and drive coil are placed in a tightly fitting tube

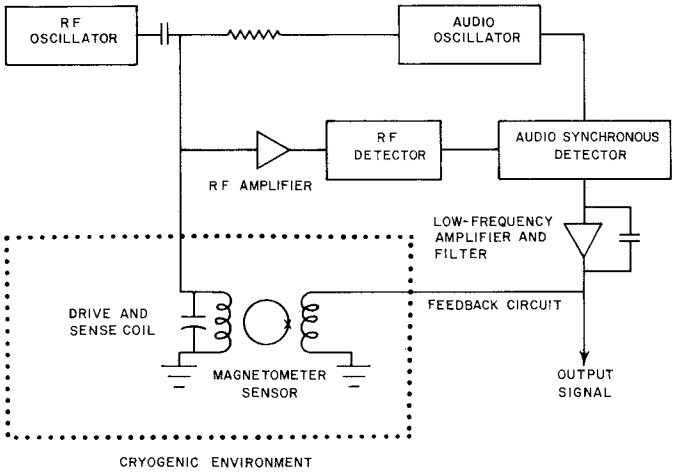

Figure 7.12. *Block diagram of the circuitry for a RF-driven Squid magnetometer (from Goree and Fuller, 1976).*

on which the superconducting field coil is wound. This assembly is then placed in a superconducting shield to isolate the sensor from all magnetic field changes except that from the field coil. The field coil of the standard sensor requires a current of about 0.3 μA to change the flux linking the Squid by one flux quantum, which is a field change of 1 γ for a 1.6-mm diameter sensor. Typical sensors are capable of a resolution of one part in 1500 of a flux quantum. Thus the peak-to-peak current resolution is 0.2 nA, which gives a field sensitivity at the sensor of 7×10^{-4} γ.

Digital Data Acquisition Systems

Digital recording on magnetic tape of the total field and doppler and altitude information is now the standard data acquisition technique for aeromagnetic survey data, and this permits the subsequent compilation of the digital data to be carried out using the computer.

For a description of the various digital data acquisition systems in current use in the industry, the reader is referred to the annual reviews published by Hood during the review period (see for instance Hood, 1972, 1973, 1976, 1977).

DIGITAL COMPILATION OF AEROMAGNETIC SURVEY DATA

Great progress has been made in the last decade in digital compilation techniques and all the major airborne geophysical survey companies now possess their own in-house computer hardware and software capability. This has come about partly as a result of the introduction of optical absorption magnetometers which required digital-recording systems to avoid the dynamic range recording problem with high resolution data, and of a general realization of the fact that digital compilation techniques would produce more objective results and would permit much greater versatility in data processing operations.

Fifteen years ago with the fluxgate and proton precession magnetometers then in use, a paper strip chart about 25 cm in width provided adequate resolution for recording the aeromagnetic field variations. However, with such a chart calibrated to allow the trace to be read to the precision of the instrument, the chart datum would be automatically reset perhaps 20 times in covering a very large anomaly, making the chart difficult to read in high gradient areas.

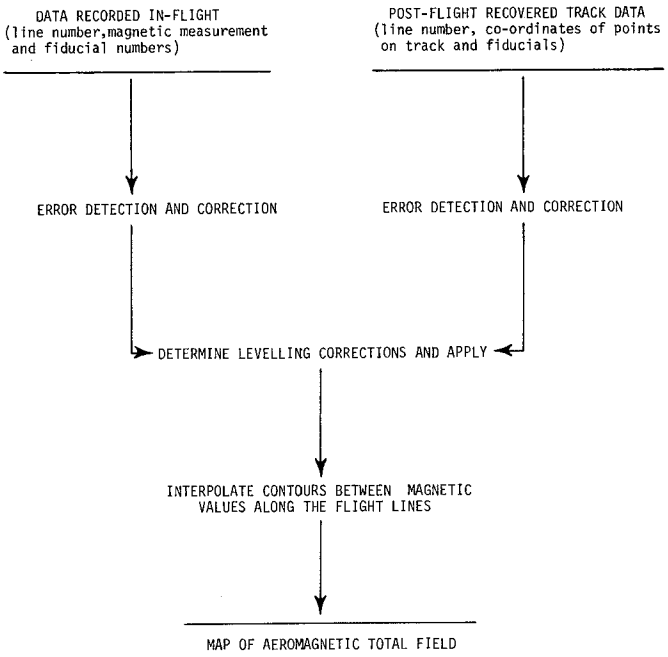

Figure 7.13. *Basic processes of aeromagnetic compilation.*

With the advent of the high sensitivity optical absorption magnetometer, the use of paper recording charts became altogether impractical. Were a strip chart recorder to be calibrated so as to be readable at the full sensitivity of an optical absorption magnetometer, then over a large anomaly the datum on the chart would be reset as much as 1000 times, producing an unusable record.

It therefore became necessary to employ a recording medium whose sensitivity matched that of the new magnetometer, and one advantageous for the less sensitive instruments. A digital recording system has, for all practical purposes, an unlimited sensitivity. This phenomenon of a need to change from analog to digital methods was not, of course, restricted to aeromagnetic work. It was widespread throughout the whole of the science and technology sector. The reason was that, although the early digital systems were more expensive than analog ones, each increase in sensitivity by an order of magnitude required a small fixed cost for a digital system ("add one more digit") whereas the increase for an analog system may require a corresponding order of magnitude increase in cost ("make the chart paper and recorder ten times wider"). A further potential advantage was offered by the lower weight, and fewer moving parts of principally electronic devices. Thus direct inflight digital recording began to be adopted by the aerogeophysical survey industry and the need for digital compilation systems arose.

Figure 7.13 summarizes the main processes of aeromagnetic compilation whether manual or digital. The levelling process removes the nongeological datum variations from line to line caused by inexact flight altitude, diurnal variation of the earth's magnetic field and other causes.

In the manual compilation process, magnetic values at the intersection points of a "levelling network" formed by the control and the main traverse lines were picked off the analog chart. Levelling adjustments were determined manually and the adjustment values marked on the analog chart at the intersections of the control and traverse lines. These points were then joined by straight lines drawn on the chart to establish a corrected datum. The magnetic profiles were then intercepted at the map contour interval required,

usually 10 γ, using the datum. These intercepted values were then transcribed onto a flight path manuscript and hand drawn contours visually interpolated between the flight lines. With the advent of digital recording, computer programs were developed to carry out those manual operations previously performed on the chart. A minimal software system would require a routine to retrieve the value of the magnetic field at the manually determined levelling network points, a routine to make a linear interpolation between these points to produce the computer equivalent of the chart datum, and a routine to output corrected values as the difference between the originally measured value and the datum at the required contour interval. These values could then be transcribed onto the flightpath manuscript and contoured manually as before.

Once having been required to employ the computer, the advantages and indeed necessities of developing beyond this minimal software system became obvious. An early requirement was the need to be able to determine errors and aberrations in the digitally recorded data. Compared with the highly visible trace on the strip chart, errors in the digitally recorded data were less easy to detect.

The most direct and familiar way to present the data for inspection being the form in which it had previously been recorded, namely, as an analog profile, development moved into the field of computer graphics. This allowed the digital data to be output in analog form and inspected for obvious errors in exactly the same manner that the strip chart had been treated previously.

Access to computer graphics having been gained, the obvious next step was automation of the laborious transcription process. This, however, would have resulted in an awkward hybrid process unless the base map of the flight path could also be produced by computer.

Another necessity then presented itself, namely the need to employ digitizing facilities. Although recovered by manual methods, flight path data once digitized, can be submitted to computer automated processes and the transcription of the data to the flight path base map made completely automatic.

Up to this point the production of computer automated compilation software had been a relatively straightforward process, the level of software sophistication required being relatively low. At this point however the required complexity of the software increased significantly.

The acquisition sequence of the in-flight data, and therefore the order of the data on the magnetic tape, is determined by logistical and economic considerations. Lines are not flown all in the same direction and in strict geographical order across the survey area as this would require a prohibitively high proportion of nonproductive flying merely to position the aircraft for each survey line. The sequence of digitization of recovered flight path data is likewise governed by practical considerations. Unless the map area of the survey at the recovery scale is small enough to fit onto the digitizing table, then flight lines must be digitized map sheet by map sheet. Hence a line which exists on the in-flight data tape as a continuous unbroken sequence of records, will exist on the digitized flight path data tape as a series of map sheet-sized segments separated by segments of other lines. In order to bring the two data sets together, it is necessary to submit them, either or both, to a complex "sort-merge" process. Once software for this purpose has been implemented, then automatic transcription of in-flight data onto flight path base maps can be carried out.

All the previously mentioned processes, though complex in some cases, are eminently suited for computer automation, consisting as they do of a sequence of well defined and repetitive processes. Such is not the case with the levelling and contouring stages.

Although the basics of the levelling process can be well defined many further factors dependent upon the skill and experience of the map compiler enter into the process as it is executed. The compiler will seek sources other than the data immediately at hand to explain and resolve dubious levelling corrections. Certain results will not "feel right" to the experienced compiler and special attention would be paid to these cases. The computer is not, of course, capable of such beneficial digressions from the specified task.

Gridding and Contouring

Similarly in the case of contouring, although the computer is capable of doing an excellent job with properly sampled data, if the data are undersampled (e.g. if the flight line spacing is too wide for the chosen flight altitude) then the computer does its best to produce a map which best represents the data as sampled – namely a poor map. With hand contouring the draughtsman would decide upon an appropriate trend and string the contours along this trend as though they were smoothly and well defined along their length. The resulting product has a pleasing, albeit potentially deceiving, appearance.

Figures 7.14a, b, c demonstrate just how appearances can be deceiving. All three maps are computer-contoured segments of an aeromagnetic gradiometer survey flown at 500 ft. (150 m) altitude with 500 ft. (150 m) line spacing. They all cover the same area of the survey but Figure 7.14a was contoured from all the original data. Figure 7.14b was contoured from every second flight line only and Figure 7.14c was contoured from every fourth flight line only. Hence Figures 7.14b and 7.14c represent the end product as it would appear had the survey been flown at 1000 (305 m) and 2000 ft. (610 m) line spacings respectively.

It must be noted that the gridding and contouring programs employed ensure that the contour positions are exact to within 0.01 cm where the contours pass over the flight lines. The contour positions between flight lines are somewhat conjectural whether contoured by man or machine, but with undersampled data, manual contours appear more reasonable. Figure 7.14c clearly exhibits the typical, undesirable features of machine-contoured, undersampled data. Namely isolated "potato" anomalies (or magnetic boudinage) elongated at right angles to the flight lines and the tendency for contours which cross several flight lines to undulate between the flight lines rather than link up the flight line contour intersection points with a smooth continuous curve, as is the case with manual contours.

Figures 7.14a and 7.14b, however, do not clearly exhibit the symptoms of undersampling. In both cases, contours cross the flight lines as smooth continuous curves and elongated trends are shown at sharp angles to the flight line direction – symptomatic of good sampling.

The interesting consequence is, however, that the 500 ft. (150 m) line spacing, which we will regard as the accurate depiction of the magnetic field variations, shows a series of four-parallel "ridges" separated by "troughs" running approximately 15° east of north, whereas the less well sampled data in Figure 7.14b exhibits only one such, but stronger, feature with a very emphatic cross-cutting trough oriented about 20° west of north. This feature is clearly spurious, but so well defined by the data as sampled that both man and machine would confidently depict it as such.

This example should leave no doubt as to the need for adequate sampling in aeromagnetic surveys. The presence of such a cross-cutting feature could be very misleading to the interpreter with potentially costly results, if, for example, it occurred in an area where economic mineralization was associated with cross trend faulting and it became the subject of exploratory drilling.

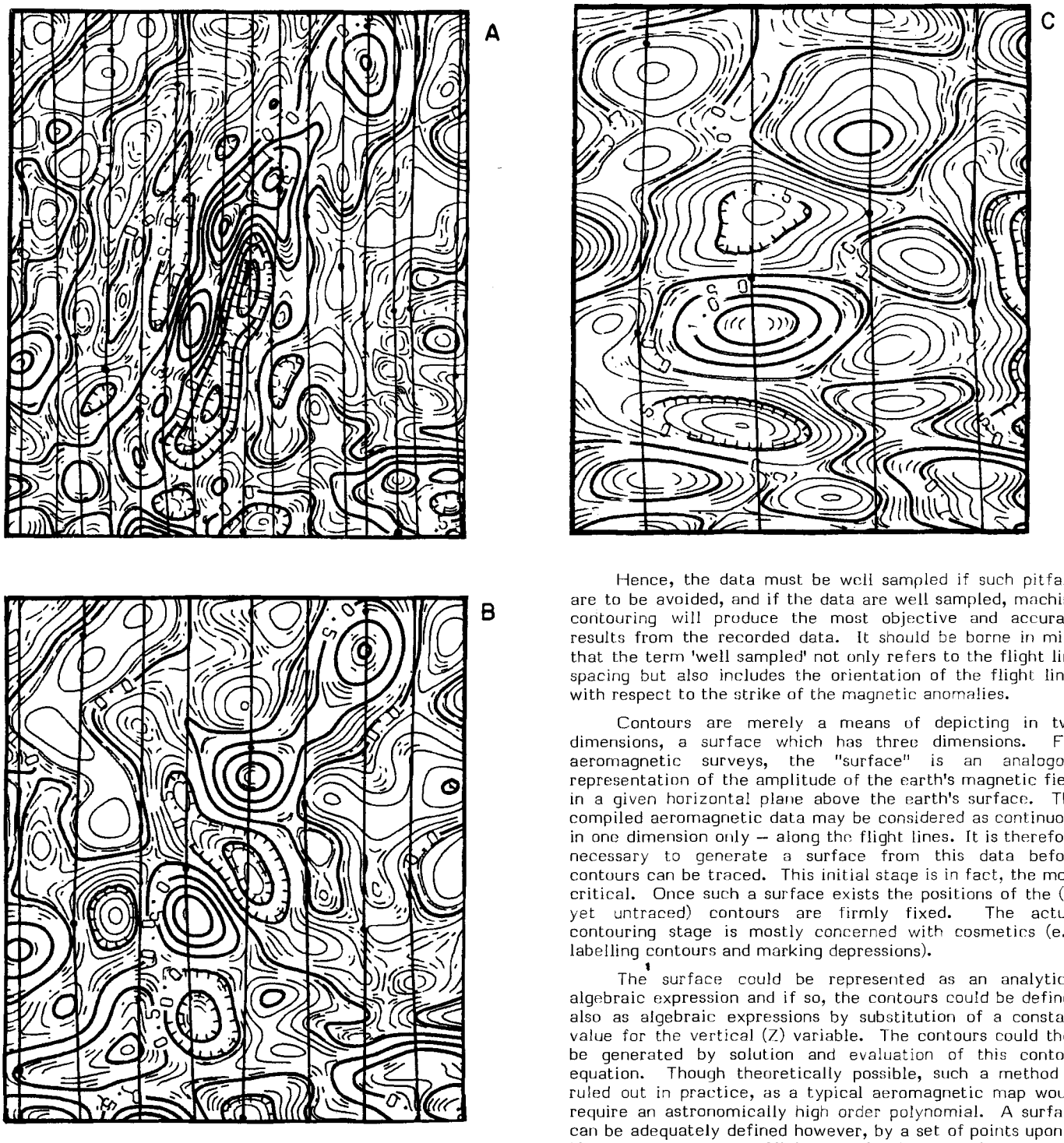

A) 500 ft. (150 m)
B) 1000 ft. (305 m)
C) 2000 ft. (610 m)

Figure 7.14. *Computer-contoured segments of an aeromagnetic gradiometer survey flown at 500 ft. (150 m) altitude in southeastern Ontario.*

Hence, the data must be well sampled if such pitfalls are to be avoided, and if the data are well sampled, machine contouring will produce the most objective and accurate results from the recorded data. It should be borne in mind that the term 'well sampled' not only refers to the flight line spacing but also includes the orientation of the flight lines with respect to the strike of the magnetic anomalies.

Contours are merely a means of depicting in two dimensions, a surface which has three dimensions. For aeromagnetic surveys, the "surface" is an analogous representation of the amplitude of the earth's magnetic field in a given horizontal plane above the earth's surface. The compiled aeromagnetic data may be considered as continuous in one dimension only – along the flight lines. It is therefore necessary to generate a surface from this data before contours can be traced. This initial stage is in fact, the most critical. Once such a surface exists the positions of the (as yet untraced) contours are firmly fixed. The actual contouring stage is mostly concerned with cosmetics (e.g. labelling contours and marking depressions).

The surface could be represented as an analytical algebraic expression and if so, the contours could be defined also as algebraic expressions by substitution of a constant value for the vertical (Z) variable. The contours could then be generated by solution and evaluation of this contour equation. Though theoretically possible, such a method is ruled out in practice, as a typical aeromagnetic map would require an astronomically high order polynomial. A surface can be adequately defined however, by a set of points upon it if the points are sufficiently closely spaced. Such a "numerical surface" is a viable alternative to the impractical algebraic surface.

Holroyd and Bhattacharyya (1970) employed a hybrid method which used a numerical surface to define the coarse features of the data. Individual algebraic surfaces were then fitted within each cell of the numeric surface for the definition of fine detail.

The potential advantage of this approach is a reduction in the amount of data required to define the surface. Only the coefficients of the polynomial defining the surface in each coarse cell need be sorted. When a pair of points on the surface are needed to fix the position of a contour, the polynomial is evaluated at these points only, thus obviating the storage of redundant surface points which will not be required to define a contour position. Although this method was originally intended for application to aeromagnetic data, subsequent evaluation showed that it was in fact particularly unsuited to aeromagnetic contouring due to the following reasons:

i) In order to realize its potential advantage, the coarse grid of the numerical surface must be fairly large compared to the fine grid that is eventually evaluated to define the contours.

ii) The coarse grid cells must be rectangular and as nearly square as possible.

iii) Aeromagnetic data are not sampled at points falling upon a regular grid. They are sampled along approximately equispaced subparallel lines at intervals five to fifteen times smaller than the line spacing.

Thus the coarse grid points will not normally fall upon a sampled point and although the grid size may approximate to the line spacing, it will have to be significantly larger than the sample interval along the lines. This means that a two stage interpolation process is required to create the contourable surface – firstly to interpolate values at the coarse grid points; secondly to interpolate the fine grid values. As a result the contours as traced generally will deviate substantially from their correct flight line intercept point and furthermore, much fine detail will be lost.

Much more effective gridding systems have been subsequently devised. The methods used by the Geological Survey of Canada and those of the Canadian aerogeophysical survey industry are essentially the same.

In general the method involves fitting smooth, continuous interpolation functions along parallel lines normal to the flight line direction. Each function has values equal to the magnetic measurements on the flight lines at the points where the two sets of lines intersect. The interpolation function lines are spaced apart at an interval equal to the ultimately desired fine grid interval and the functions are evaluated along these lines at points separated by the same interval, thus producing the fine grid directly.

By this method the contours when traced pass within 0.01 cm of their true flight line intercept position and all fine detail is preserved. The desirability of such a result far outweighs the minor disadvantage of having to calculate values at every fine grid point even though many of such values may not be required to fix a contour position. Even this necessity becomes an advantage if further digital processing, such as digital filtering, is to be applied as such processes require values at all grid points.

As noted, once a numerical surface defined by a closely spaced grid has been created, contour positions are fixed. The Geological Survey of Canada and the Canadian aerogeophysical industry have adopted a general standard square grid interval of 0.25 cm measured on the contour map.

Thereafter the actual "contouring" programs are mainly concerned with matters such as contour labels, line weights and feathering of lower order contours in high gradient areas. These cosmetic processes however should not be underestimated as, in the better programs, the complexity and sophistication of the algorithms required exceed that of many other stages of the compilation and cartography processes.

Most aeromagnetic maps currently produced in Canada for the federal government by aerogeophysical exploration companies or by the Federal Government itself are now machine contoured. This is feasible because the survey specifications ensure adequate sampling of the magnetic field and hence allow a machine-contouring package to do its work with little difficulty.

Figure 7.15 shows a flow chart of a digital aeromagnetic compilation system similar to the one in use by the Geological Survey of Canada.

Several stages are annotated as being optional. The digital filter stage for example, need not be applied to aeromagnetic total field data except to remove high frequency sampling noise (without distortion of the geological anomalies) if such is present. The extraction of the levelling data set and the application of level adjustments, are not necessary for aeromagnetic gradiometric data. Such data are presently levelled using a digital filter which removes any long-wavelength variation from the profiles. Thereafter the data, as they are not subject to diurnal variation, should be contourable without further levelling adjustment.

The derivation of alternative data forms is also an optional process. Some of the alternative forms that can be produced are for example regional or residual maps, vertically continued maps, and derivative maps.

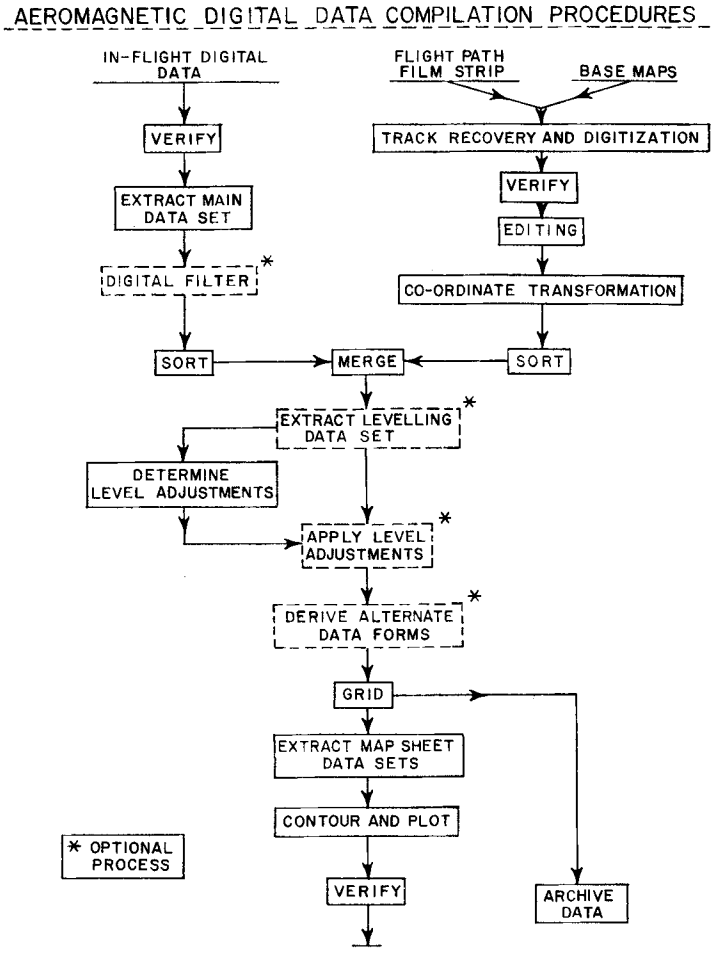

Figure 7.15. *Flow chart for digital aeromagnetic compilation system.*

Levelling methods however are still not totally automated. Some Canadian companies and the Federal Government use entirely automatic methods, others rely upon manual methods and yet others on a hybrid technique. Current trends in development in computer software and automated methods however are making it easier to decide between fully automated and manual methods.

The trend referred to is the increasing use of interactive systems rather than the previous almost universally used batch system. With an interactive terminal (preferably a graphics terminal) on line to a computer service bureau or as a peripheral of an in-house computer system, those parts of the work best done by the computer can be automated, and those parts requiring human interaction can be presented to the map compiler via the terminal. Such a system obviates the time consuming need to switch from a manual to a batch process and back again with the attendant problems of interfacing between the man and the machine.

With such a system, applied to levelling for example, the clearly defined processes of the levelling can be carried out on the computer at its own very high speed. When a problem arises that cannot be resolved by the computer algorithm the computer can then present the information to the compiler at the terminal for his inspection and decision as to the best course of action. After the decision is made the computer can continue until another similar decision point is reached.

Work currently in progress at the Geological Survey of Canada includes investigation of methods which will eventually allow the interactive process to be applied to contouring. The data will be contoured and the contours presented to a compiler at a graphics terminal. If the data appear to have been adequately sampled and the automatically produced contours are acceptable, then no action by the compiler will be required. If however the data are undersampled and trends, which are visible to the compiler, are inadequately depicted by the machine contouring, then the compiler, by use of a graphics input device, will be able to indicate to the machine the linkages to be made between spuriously isolated anomalies. After this the machine will recontour the data enforcing the appropriate trending of contours across the map. After every session of automatic contouring, the data will be presented to the compiler until final acceptability has been reached. After this the contours can be output in final form on a digital plotter.

Error Detection

The most time-consuming stages of the compilation process are the verification of the in-flight data and the track data. Identification and removal of data errors and abberations are vital if time-consuming reprocessing is to be avoided.

Both the in-flight and the recovered track data set are subject to a great variety of types, and degree of severity, of man and machine errors. If, for example, either the in-flight instrument operator or the digitizer operator miskeys a line number, then a lack of correspondence between the two data sets will arise at the sort-merge stage. An even worse situation is when line numbers are somehow transposed. All lines of in-flight data would have a corresponding line of track data and thus the error could remain hidden up to the levelling or even final contouring stage. As well as such gross logical errors, many physical errors are encountered. With flight path data, a recovered point may be inaccurately positioned on the recovery map or its position may be inaccurately digitized. Means exist, however, to detect automatically severe cases of such errors (and also the logical corollary, where a track point is correctly positioned but mislabelled).

The principal error detection method is known as a "speed check", and was also employed in manual compilation; the technique has been adapted with much improved sensitivity to digital compilation. The time at which each recovered track point was flown over is known. From this information and the positional co-ordinates, the speed-check program calculates the apparent speed of the aircraft between each pair of track points. The actual aircraft speed will vary but this variation should be smooth i.e. no sudden significant changes in speed. If a track point is misplaced, for example, some distance along the direction of flight then the track segment before this point will be lengthened and the one after shortened. As the time of passage over these points will not have changed this causes an apparent increase in speed before the point and a corresponding decrease after it. If the positional error is significant, the apparent change in speed at the misplaced point is readily detectable and the error clearly indicated. Without such a check, the contours would be distorted in the vicinity of the misplaced point.

Physical errors in the in-flight data set stem from two principal sources: malfunction of either the sensing or the encoding-multiplex-recording system and to such effects as miscompensation of the airborne magnetometer system to aircraft motions. Figure 7.16a shows the four ways in which these errors manifest themselves in the data. The first three, spikes, steps or hash are high frequency features; the last, drift, is a medium to low frequency feature. At any given distance from a magnetic body, there is a calculable minimum width to the anomaly it causes. This minimum width increases as the distance from the body. At the usual flight altitudes and with the usual measurement frequency, the minimum anomaly size is several measurement intervals wide since the measurements are normally spaced about 75 m (250 ft.) apart on the ground for aeromagnetic surveys.

Thus features in the magnetic field record defined by a single point or several single point features in succession — such as spikes, steps or hash — are clearly erroneous and can be detected and corrected at the earliest stage of compilation.

Low or medium frequency drift, however, possesses the same frequency characteristics as genuine anomalies and usually remains undetected until the levelling or even contouring stage is reached. Even though detectable, very little can be done about it as the drift and the genuine anomalies upon which it is superimposed, are inseparable. The best that can be done is to discard that section of the data containing it.

The high frequency errors present a much more tractable problem. High frequency noise detection programs were recently added to the ADAM system (Holroyd, 1974) which is employed by the Geological Survey of Canada for the autocompilation of aeromagnetic and airborne gradiometric data. These programs are designed to find and remove spikes, the most common form of error, and to indicate the presence of steps and hash. The kernel of the process is a routine to recognize general disturbances and certain specific patterns in the fourth difference of the data values.

As the values are equispaced the fourth differences, about the i^{th} data element, d_i, is given by the expression (see Fig. 7.16b):

$$d_{i+2} - 4d_{i+1} + 6d_i - 4d_{i-1} + d_{i-2}$$

As can be seen, the expression involves the five consecutive data values centred upon the i^{th} value and the error in d_i would be amplified by a factor of 6 with the same sign; adjacent fourth differences would have error values four times that of d_i but with the opposite sign. The fourth

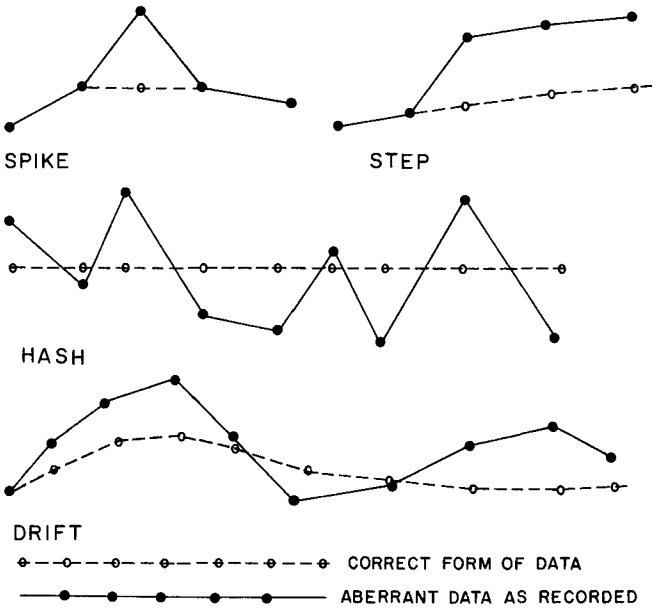

Figure 7.16a. *Commonly encountered types of error in digitally-recorded aeromagnetic survey data.*

difference is employed specifically because a true spike needs five consecutive points to define it. The first difference (slope) can be large on the sides of a spike but it could be even steeper on a genuine anomaly. The second difference can be large on the point of a spike but can also be large naturally, similarly for the third difference. When the fourth difference is reached, its value over all the correct and smooth parts of the data tends to zero, but the value over a spike becomes very large.

With "hash" every point can be considered as a spike and consequently the fourth difference tends to multiply the hash swath by a factor of 2^4, i.e. 16 (see Fig. 7.16b). The actual fourth difference pattern would not be significant if the intent was merely to locate aberrant data of any of the high frequency types. The intent, however, is to separately identify spikes. This is because spikes are the most common of the three types of high frequency aberrations, and unlike the other two, are simple to correct automatically. To this end, the program seeks not only for high values of the fourth difference but also for the special patterns of variations within the fourth difference which typify the spikes and step. For the spike, this pattern is five consecutive fourth differences whose values are in the ratio +1:-4:+6:-4:+1 and the waveform is symmetrical about the error point (see Fig. 7.16b). To eliminate the spike in the original data using a fourth-difference table, the two fourth-difference (4 x error e) values on either side of the symmetrical peak are first averaged and then added to the fourth-difference peak (6 x error e) value to give a resultant which is ten times the spike error e in the original data. The appropriate value in the original data corresponding to the position of the peak in the fourth-difference values is then corrected using one tenth of the calculated 10 e value. For the step the pattern is four consecutive values in the ratio +1:-3:+3:-1 (see Fig. 7.16b) so that the resultant waveform is antisymmetrical about the error point. This test is extremely sensitive and in use it has revealed genuine spikes of such a low amplitude that their presence in the data was previously unsuspected. Due to the precision and smoothness of high sensitivity data, it has been possible to detect spikes of 0.1 γ in data with very high gradients and high frequency anomalies of over 10 000 γ amplitude.

The advent of interactive processing systems has greatly speeded up quality control of the work. The practice of verification on an interactive system varies significantly

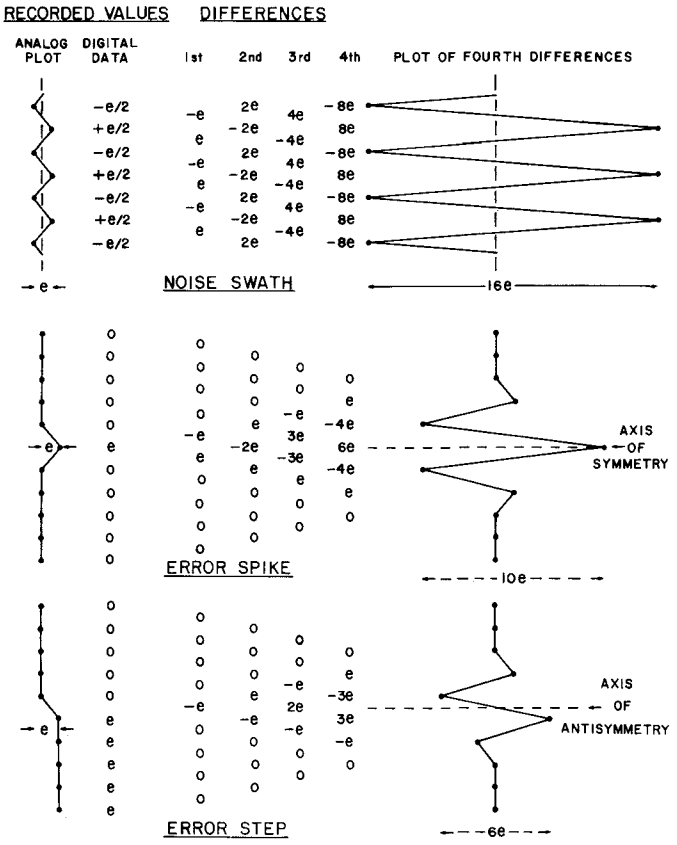

Figure 7.16b. *Amplification of errors by calculating fourth differences and the resultant waveforms of the plotted fourth differences.*

from that on a batch system. With a batch system where no human interaction takes place, it is necessary to pre-define the boundary between acceptable and unacceptable data. As it is almost impossible to predict in advance exactly the types of error to be encountered, it is necessary to make the error-detection routine "over zealous". That is, it is necessary to accept misidentification of good data as bad, rather than allow bad data to be accepted as good. This means that a batch system will not only correctly identify genuinely erroneous values, but it will also identify a significant quantity of valid data as invalid. This then requires detailed, usually manual, work to separate the true errors from the spuriously identified ones.

The nature of interactive systems allows a much more effective method to be applied. Namely, three classes of data are defined. Firstly the data which are clearly wrong, lastly the data which are clearly correct, and in between the two extremes a grey area is defined where the data are suspect but not clearly right or wrong. A batch-processing program can be used to separate the data into these three types. The clearly erroneous data may be processed automatically, the clearly good data may be passed on without any further attention, but the data falling into the grey area between the two may be reserved by the system for interactive inspection. Thereafter a compiler seated at a graphic or other type of terminal can make the decisions regarding acceptability or non-acceptability of the data, a task which the human being can do far more effectively than the computer.

Such a system, incorporating the above mentioned "spike finder" has been implemented at the Geological Survey of Canada. A batch program detects disturbances in the

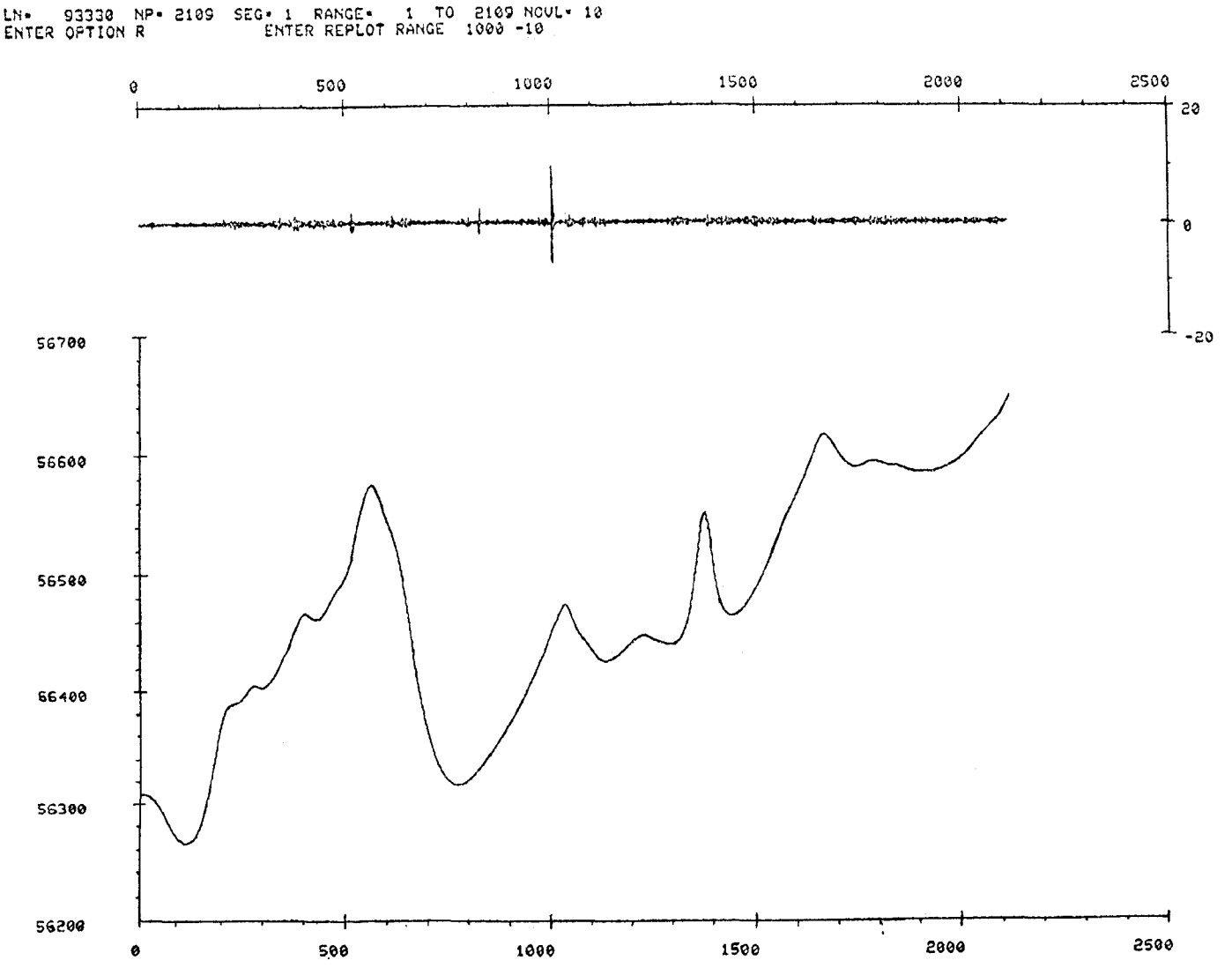

Figure 7.17. *Data inspection by interactive graphics.*

fourth difference of the data, clearly defined spikes are automatically removed, and those segments of the data containing disturbances, whether spikes or other types, are reserved on a disc file for later access by the interactive program.

Figures 7.17 and 7.18 show examples of interactive viewing of data set aside by the batch program. The graphs, axes and fine print text are a photograph of the actual graphics terminal hard copy unit output, i.e. what was actually displayed on the screen. Figure 7.17 shows the initial display for a segment of data together with a graph of the fourth difference values above. The y axes units are those of the data or fourth difference values, the x axes units are simply the number of the data point with respect to the first data point in the displayed sequence. The data profile has a range of over 400 γ on the y axis and contains 2109 data points. It is as smooth as the resolution of the graphics screen permits. The fourth difference profile however shows several spikes, the largest of which according to its position on the x axis, lies somewhere in the vicinity of the 1000th point in the sequence. After plotting the graphs, the compiler may select that part of the data containing the spike and display it on the screen.

Figure 7.18 shows the resultant display in which 10 points on either side of 1000 have been selected. The specified segment is replotted and as it covers only 20 points with a y axis range of only 17 γ, the 1.6 γ spike which caused the original disturbance in the fourth difference becomes clearly visible. It should also be noted that the amplitude of the spike can be calculated from the upper trace in Figure 7.17 by dividing the peak-to-peak fourth difference signature by 10. It should be noted that the basic noise level of the aeromagnetic survey system can be calculated from the upper trace of Figure 7.17, by dividing its width by 16. In this example the noise swath is estimated to be approximately 0.1 γ.

As to future development, Dutton and Nisen (1978) noted that during the 1960's the emphasis was on hardware. This for the aerogeophysical survey industry meant the period during which the new magnetometers and digital recording equipment plus the digitizing tables and computer graphics devices came into use. The writers stated that during the 1970's the emphasis was on software. This for the aerogeophysical industry was the development of the digital compilation systems which are now almost universally in use throughout the industry. Finally, the prediction for the 1980's

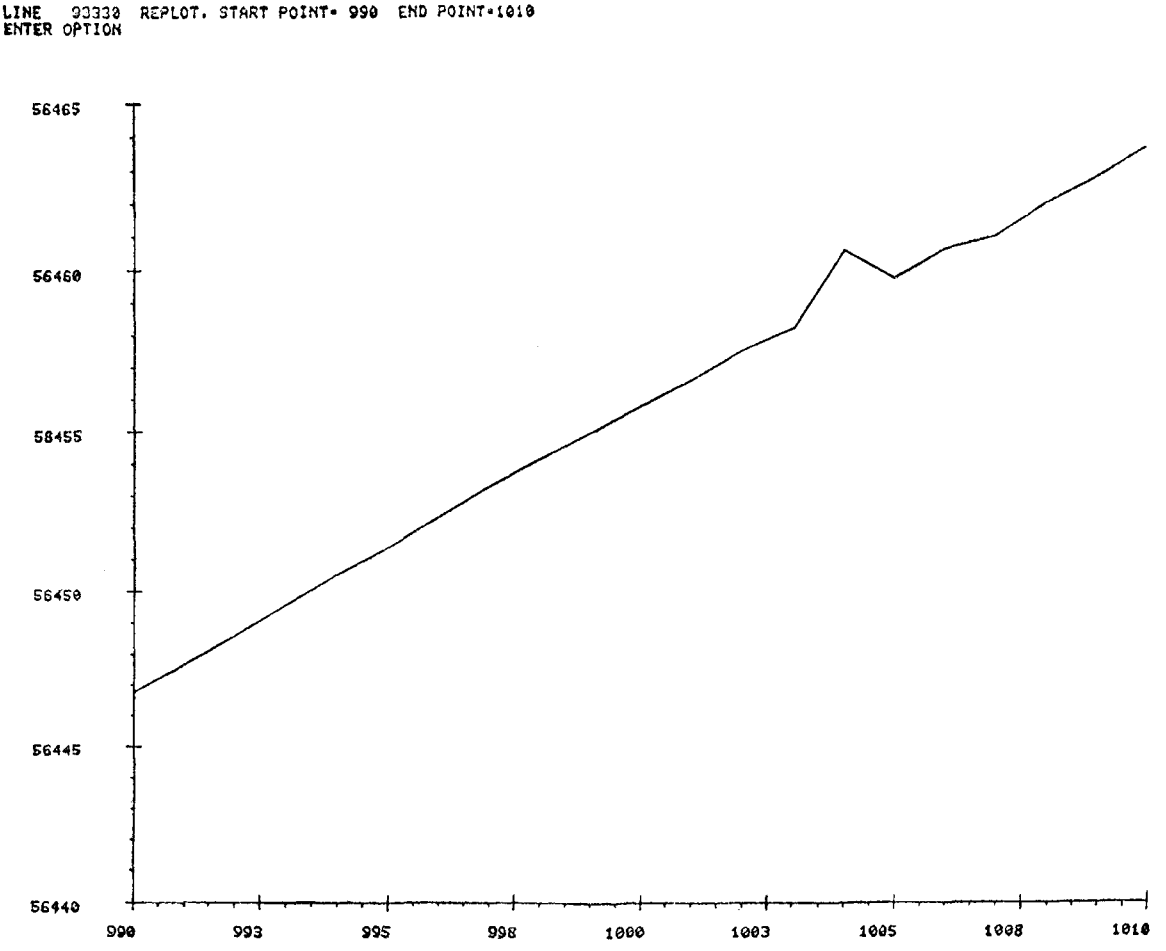

Figure 7.18. *Amplified replot of that part of the aeromagnetic profile presented in Figure 7.17 in which an error spike occurs.*

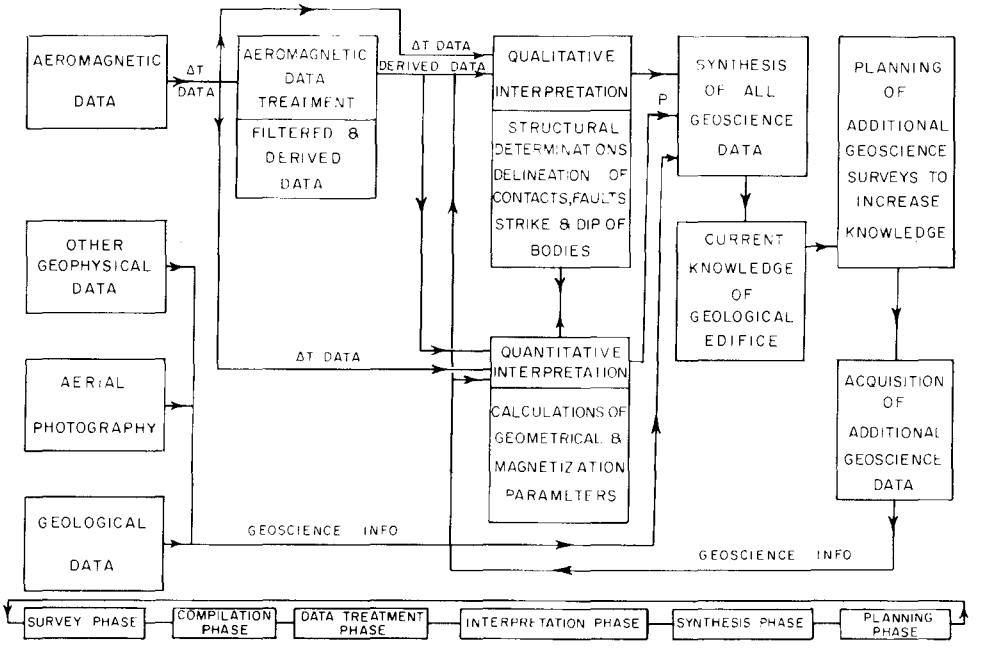

Figure 7.19. *General scheme for the interpretation of aeromagnetic data.*

was that the emphasis will be on data bases. One could interpret this with respect to the aerogeophysical industry as meaning that now the data are digitally recorded and processed by mainly automated means, the question remains as to what to do with the ever increasing quantity of digital information on hand. The aeromagnetic digital data bank of the Geological Survey of Canada already costs several thousand dollars per annum merely for rental and storage of the digital tapes upon which it resides. It is evident that, as the quantity of data continues to increase and more and more methods are developed for further usage of this valuable resource, then more sophisticated means will have to be developed to retrieve and further utilize this data.

DATA PROCESSING

Advances in data processing techniques during the past decade have mostly involved the application of digital data filtering techniques and power spectrum analysis (see Spector and Grant, 1970) in order to emphasize the higher frequency components of the crustal field and remove the regional gradient of the earth's magnetic field and the longer wavelengths of the crustal field. Because of space restrictions, the topic is left to the paper in this volume by Spector and Parker (1979) for a more comprehensive review.

Several techniques for determining the magnetization or effective susceptibility of underlying rock formations were developed during the past decade all of which may be considered to be a form of filtering. Bott and Hutton (1970) published a technique for use on profiles in which the depths to the top of the magnetic formations had to be known. O'Brien (1970) has reported on an inverse filtering technique which combined pole reduction with downward continuation in order to transform the anomaly due to a magnetic dipole into a narrow spike. It was claimed to be effective in locating contacts and in outlining areas of higher magnetization contrasts.

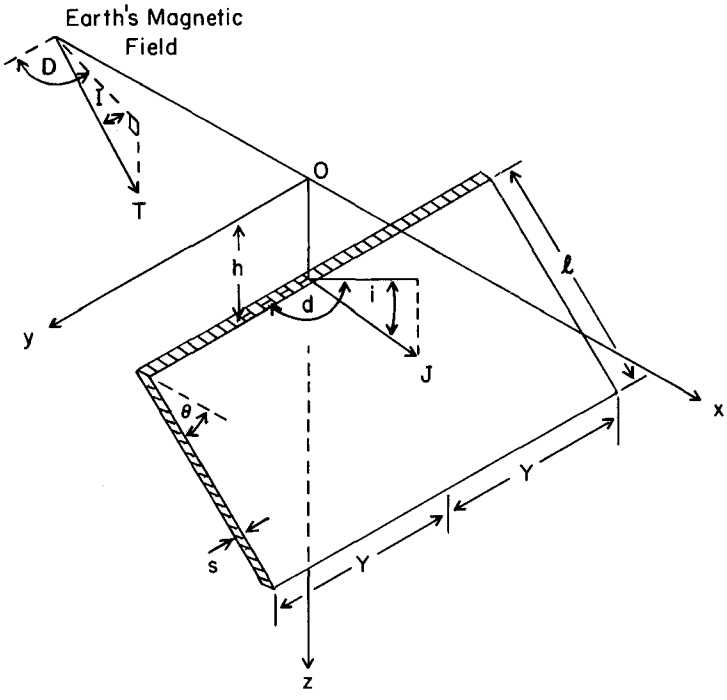

Figure 7.20. *Oblique view of thin plate showing nomenclature used (from McGrath and Hood, 1973).*

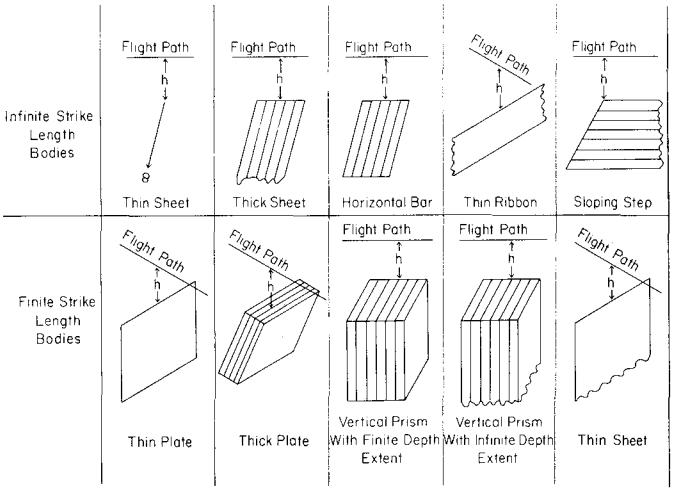

Figure 7.21. *Geometrical models that may be generated from the thin plate model by numerical integration (from McGrath and Hood, 1973).*

In 1973, Paterson, Grant and Watson Ltd. of Toronto developed a new technique for the interpretation of aeromagnetic maps in which the magnetic susceptibilities of the underlying rock formations are calculated (Grant, 1974). Magnetic susceptibility mapping assumes that the bedrock is composed of a large number of homogeneous, vertical rectangular prisms whose upper surfaces follow the bedrock topography. By generating a horizontal grid of total intensity values from the flight-line data, the magnetic susceptibilities of the prisms may be calculated directly from the gridded data through an inversion. Tandem software provides for the rectification of drape-flown surveys, for regional-residual (deep versus shallow) separation, and for final adjustment to flight-line observations if desired. The resultant magnetic susceptibility contour map is a useful tool for determining geological boundaries. It is most effective when sufficient outcrop information is available to identify the lithology of the various magnetic rock units. In such circumstances it may be used with appropriate care and caution to extend geological mapping into unmapped areas or beneath nonmagnetic cover. In the absence of such controls, the magnetic susceptibility map may be viewed as a contour presentation of the volume concentration of magnetite (or magnetite equivalent) in the bedrock. Such a map can be useful in exploration studies for making preliminary geological interpretations, and for solving special problems such as locating felsic/mafic contacts, outlining the metamorphic zones in an intrusion, etc.

AEROMAGNETIC INTERPRETATION

It is axiomatic that the ultimate value of a given aeromagnetic survey lies in the geological information that can be derived from an interpretation of the resultant data. Figure 7.19 is a block diagram showing ideally how aeromagnetic data should be interpreted to maximize their value and this can only be done effectively by using the other kinds of geoscience information available. On the left hand side of Figure 7.19 are the information inputs into the system, namely aeromagnetic data, other kinds of geophysical data, aerial photography and the geological information known about the area. First the aeromagnetic data may be treated in some fashion to improve the resolving power of the technique. Such treatment will result in some form of filtered map being produced, for instance, a second vertical derivative or downward continuation map, which emphasizes

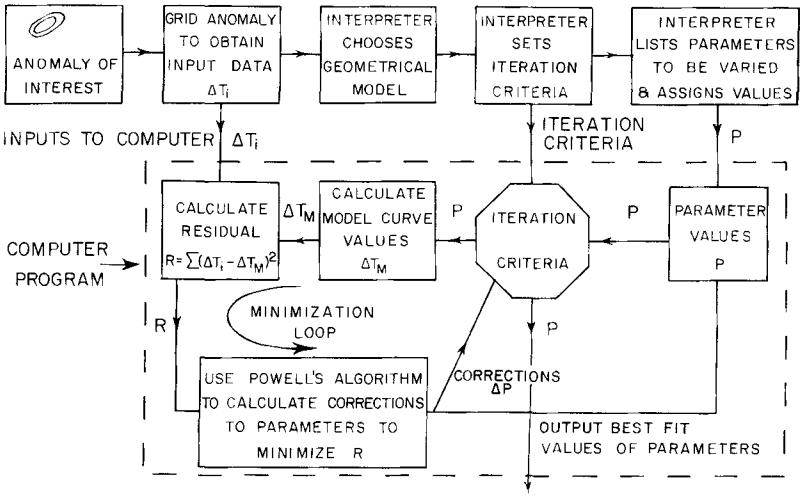

Figure 7.22. *Automated least-squares multi-model method of magnetic interpretation.*

the magnetic effects of the near-surface geology and removes the gradient effects of the main earth's field. Then the interpretation proper of the aeromagnetic data is carried out and this important step may be divided into two phases. The first phase is a qualitative interpretation in which areas underlain by a common rock type are delineated and structural features such as faults are recognized. Then a quantitative interpretation is carried out in which the geometrical shape and position of each causative body producing an individual anomaly is calculated together with its intensity of magnetization; the latter being, of course, the diagnostic physical parameter for the magnetic survey technique. The value obtained for the intensity of magnetization will be a guide to the lithology of the causative body. However, as a control on the quantitative interpretation, and to set permissible limits for the upper and lower values acceptable for the intensity of magnetization, it is recommended procedure to obtain representative remanent magnetization and susceptibility measurements of the main formations in the survey area. The results emanating from the qualitative and quantitative interpretation should, of course, be compatible, which is the reason for the arrows between these two blocks on Figure 7.19. Now, at the synthesis phase all types of geoscience information including that resulting from the interpretation of the aeromagnetic data are combined in order to deduce the most probable geological edifice for the area. At this stage it may become apparent that knowledge of the geological edifice is weak in some particular aspect and so the interpreter may recommend that additional geoscience surveys be carried out to fill in these gaps. There is a point that we particularly wish to emphasize, namely that there should be a feedback loop in the interpretation sequence. After additional geoscience information is acquired and subsequently fed back into the synthesis phase, a further interpretation of the aeromagnetic data is often worthwhile. Thus the first interpretation of the aeromagnetic data should not necessarily be considered the final one. There is always additional information which can be gleaned from the data and the acquisition of other types of geoscience information may indicate what additional facets of information can be derived from the aeromagnetic data. Thus the point of this discussion is to bring out the interrelationship between all the kinds of geoscience information useful in the interpretation, and the fact that the results from a particular geoscience discipline should not be interpreted in isolation.

Quantitative Interpretation of Aeromagnetic Survey Data

We have counted 130 articles on quantitative magnetic interpretation which have been published during the past decade so it is impossible to comprehensively review the interpretation literature in the space available for a general review. We will therefore only attempt to summarize and highlight what appear to be some of the more significant advances since 1967:

In general, the articles have been concerned with four main types of interpretation method:

1) the more classical interpretation techniques in which special points on the anomalies, such as the maxima, half-maxima, minima, inflection points etc. are utilized together with a set of charts to calculate the geometrical parameters;

2) computer depth-profiling techniques in which depth estimates are made along digitized magnetic profiles using a single or multigeometry causative body model;

3) computer curve-fitting techniques in which a three-dimensional geometrical model is derived by an optimization technique whose calculated anomaly best fits a set of gridded data in a horizontal plane; and

4) interactive computer graphics techniques utilizing curve-fitting methods in which the interpreter may communicate interactively with the computer through a CRT display and light pencil to modify the interpretation.

An example of the first type of interpretation method which does not utilize the computer, concerned the dipping-dyke case (Koulomzine et al., 1970). Their algorithm involves splitting the anomaly curve into symmetrical and antisymmetrical parts by folding but more importantly presents a quantitative technique for first ascertaining the position of the origin for the anomaly so that an estimate of the background datum level is not required. The technique then utilizes maximum, three-quarter and half maximum abscissal distances and the maximum amplitudes of the symmetrical and antisymmetrical curves together with a single master curve.

Another notable article was that by Am (1972) which presented a mathematical review of the magnetic anomalies of thin and thick dipping dykes and derives the characteristic points which can be utilized for depth estimation and presents a set of curves by which the parameters of the causative body may be calculated.

In the second group, one of the first notable articles which dealt with a computer depth-profiling technique was published by Hartman et al. (1971). They applied the so-called Werner deconvolution method to vertical gradient, horizontal gradient, and total field data in which the elemental models utilized were a single dipping sheet for a body with a thickness less than its depth or a stack of such sheets to simulate the wide block or contact case. Because the Werner equation has four unknowns and in order to reduce the effects of interference, a set of six or seven equally-spaced points were taken in order to produce a set of simultaneous equations which are solved by the computer. The entire sequence of data points was then advanced by one point along the profile and the calculation repeated. A correction had to be made for each anomaly determination if the profile did not cross the strike of the causative body at right angles or if the strike of the body was not effectively infinite.

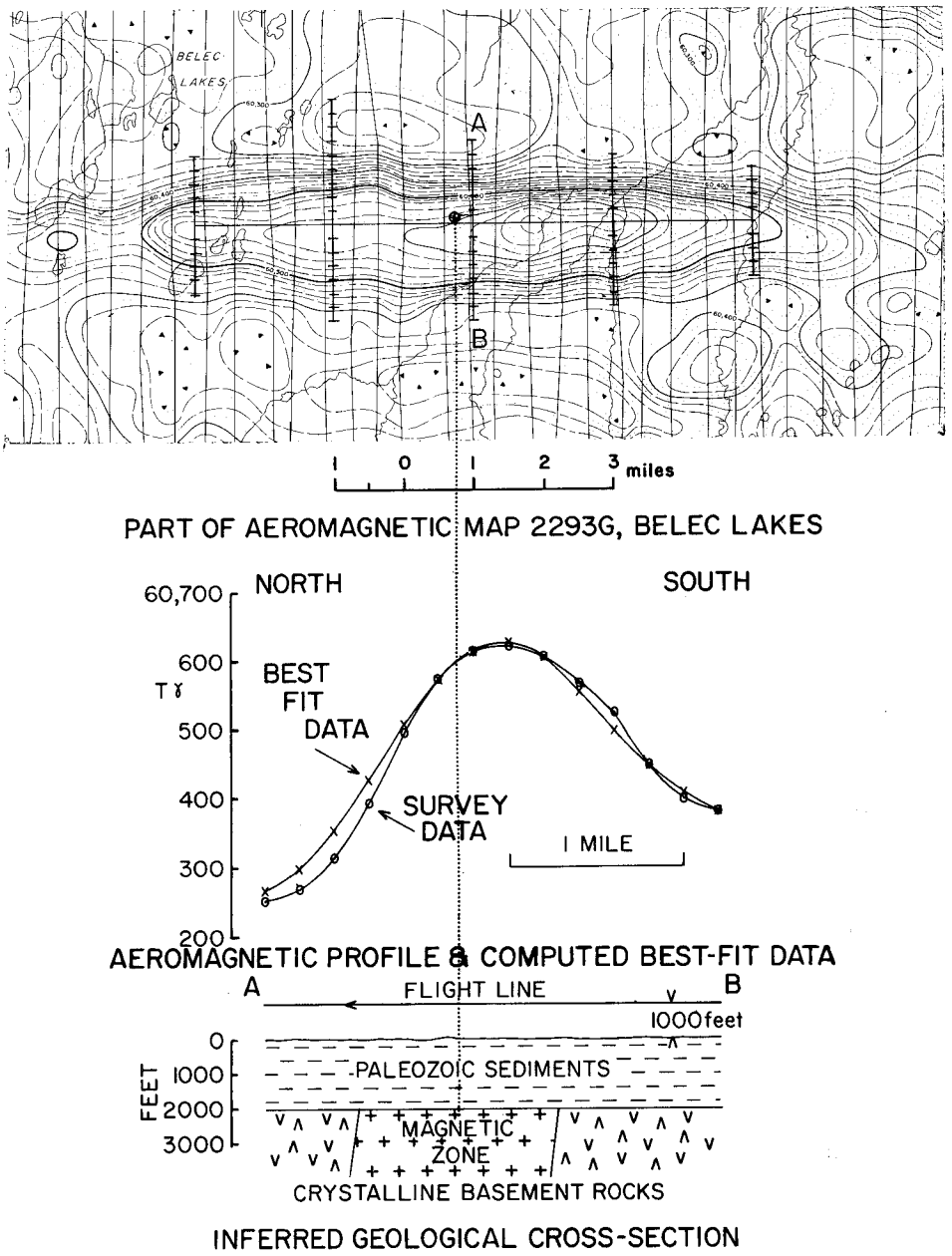

Figure 7.23. *Aeromagnetic and geological data for the Belec Lake anomaly caused by a magnetic zone in the basement rocks of the Hudson Bay Lowlands, northern Ontario (from McGrath and Hood, 1973).*

Computer curve-fitting techniques for profiles have undergone a great deal of development during the past decade and techniques have been published by Johnson (1969) for two-dimensional structures, by McGrath and Hood (1970), and by Rao et al. (1973) for the dipping dyke. These techniques differ from the Werner deconvolution technique in that a single solution for the causative body is obtained from the whole anomaly whereas in the computer curve-scanning technique a set of solutions is obtained as the computer scans along the anomaly taking a relatively small number of data points for each individual calculation.

Naudy (1971) also described a computer depth-profiling technique which utilized the dipping dyke and lens models in which an individual anomaly was split into its symmetrical and antisymmetrical components. The final result was a series of symbols placed on the chart by the computer which correspond to the depths to the tops of the corresponding model.

O'Brien (1971, 1972) developed a computer depth profiling technique, called Compudepth, for determining the edges of and depths to two-dimensional prismatic bodies. The computer algorithm employs the spatial equivalent of auto-regression in frequency space but the accuracy of the technique depends greatly upon the system noise level and magnetization contrasts.

For the third group, several articles have been published which describe a computer algorithm for the derivation of three-dimensional models whose calculated anomalies best fit

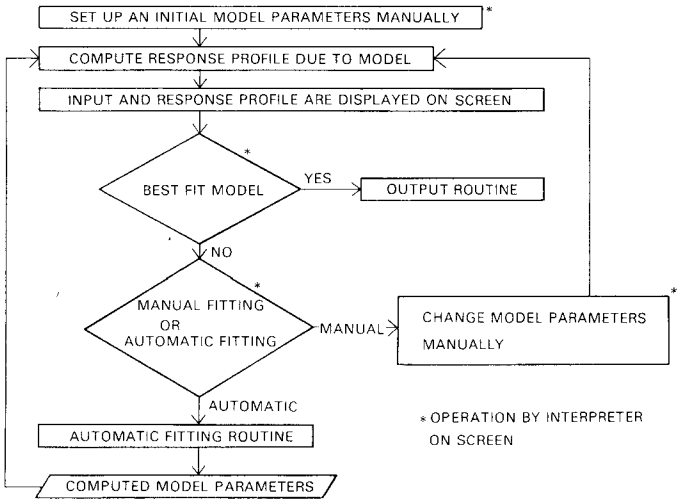

Operation flow chart of interpretation by "IMIS".

Figure 7.24. *Interactive computer graphics interpretation technique (from Ogawa and Tsu, 1976).*

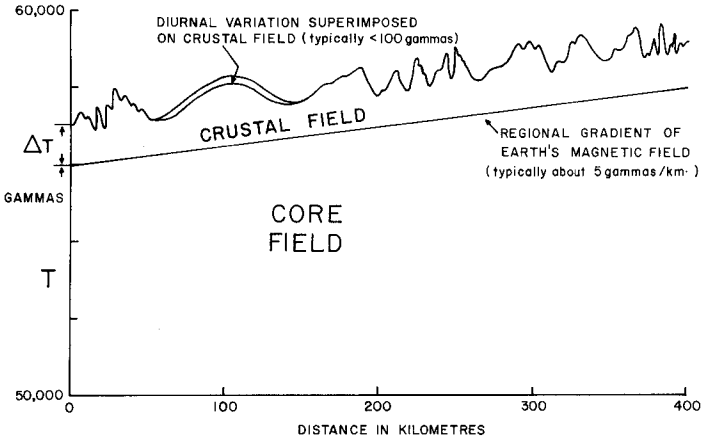

Figure 7.25. *Typical aeromagnetic profile across the earth's surface in Canada showing the contribution due to the earth's core, the crustal rocks and diurnal variation.*

the observed anomaly on a contour map. In 1973, McGrath and Hood published such a computerized curve-matching technique which utilizes a numerical integration of the equation for the magnetic anomaly due to a thin rectangular plate (Fig. 7.20) to generate an anomaly for one of the geometrical shapes shown in Figure 7.21. Figure 7.22 is a block diagram for this automated least-squares interpretation method. After selecting the anomaly of interest, the anomaly is gridded to obtain the input data. The interpreter then chooses the geometrical model that he thinks best fits the causative body based on the shape of the anomaly and other geoscience information that is available for the area. By selecting a geometrical model, the interpreter in essence selects the mathematical equation to which the input data are to be fitted by a least-squares iteration technique, and this is of course a subjective judgment. The mathematical equation for the model used contains the geometrical parameters such as the depth, width, vertical thickness and length of the causative body and also its magnetization contrast with the surrounding country rock; the magnetization is a vector, that is, it has both magnitude and direction. To obtain the values for the foregoing parameters, the computer program varies each of these parameters in turn until the best-fit criterion is obtained. Thus the interpreter has first to decide how the iteration procedure should be stopped, for instance this decision may simply be an arbitrary number of iterations. It is also necessary for the interpreter to decide the parameters that should be varied and then assign initial values which are usually obtained by simple graphical methods. These initial parameter values are fed to the computer, inserted in the equation and the resultant model curve values, which correspond with each of the input data values, is generated. Then the sum of the least-square differences between the anomaly and model curve values is calculated and an algorithm devised by Powell is used to calculate corrections to the parameters in order to minimize this least-square difference residual value. These corrected parameter values are then fed back into the equation and the process continues until the iteration criterion is reached, when the computer outputs the best-fit values obtained for the parameters. This means, of course, that the anomaly values have been fitted as closely as possible with those generated by the geometrical model using the calculated parameters.

The example selected to illustrate the use of the computerized interpretation algorithm is located in the Moose River basin of the Hudson Bay Lowlands in northern Ontario, which is underlain by Paleozoic sedimentary rocks resting on the Precambrian crystalline basement. The upper part of Figure 7.23 shows the Belec Lakes magnetic anomaly which appears on GSC Aeromagnetic Map 2293G. The contour interval is 10 γ and the survey flight lines are spaced 0.5 mile (0.8 km) apart; survey elevation was 1000 feet (305 m). The amplitude of the anomaly is approximately 380 gammas. The second set of thicker solid lines shows the position of the sampling grid which was placed over the anomaly. These consist of 5 profiles such as AB along each of which 9 to 17 sampling points at 0.2 mile (322 m) intervals were placed; the distance between each profile is ten sampling intervals. Thus there are 63 sampling points used in the interpretation of this anomaly. The thick dipping plate model was chosen, and it was found that the least-squares fit was insensitive to the vertical thickness of the model thus indicating that the depth extent of the causative body is at least five times the depth to its upper surface. The computer determined that the best-fit width of the causative body was 5670 feet (1728 m) and its strike length was 47 000 feet (14 325 m). The calculated depth to the top of the causative body was 2960 feet (900 m) which indicates a thickness of 1960 feet (600 m) for the Paleozoic sedimentary formations and the dip of the causative body was 82° to the north. The best-fit computer values for the total intensity of magnetization vector were a dip of 64° and a declination of 107° east of magnetic north. The dip of the earth's magnetic field in this area is 79°, which means that the causative body must possess a significant remanent component of magnetization. The effective susceptibility contrast which includes the remanent component was calculated to be 2300×10^{-6} cgsu (29 kappas) which is a typical value for igneous rocks. We think that the automatic computer interpretation methods will prove of great value to the industry geophysicist if applied judiciously and enable him to interpret such anomalies more objectively than he has been able to do in the past.

As an extension of the computer curve-fitting technique, it is now possible to adapt the method using an interactive graphics terminal. Ogawa and Tsu (1976) have described such a system in which a combination of either manual or automatic curve-matching procedures may be used in interpreting profiles or contour maps (Fig. 7.24). Their automatic adjustment is based on a least-square minimizing technique which utilizes a modified form of the Marquardt algorithm.

A useful aid to interpretation was published by Andreasen and Zietz (1969) who produced a catalog of 925 theoretical anomalies for a 4 x 6 depth unit vertical prism with vertical thicknesses ranging from 0.1 depth unit to infinity. The anomalies were computed for inclinations of the earth's field ranging from 0° to 90° in steps of 15°. For each model to indicate the effects of remanent magnetism, the azimuth with respect to magnetic north and the inclination of the polarization vector were systematically varied from 0° to 90° and from 0° to 150° respectively. The resultant changes in the shape and skewness of the total field anomalies are most instructive in carrying out qualitative interpretation.

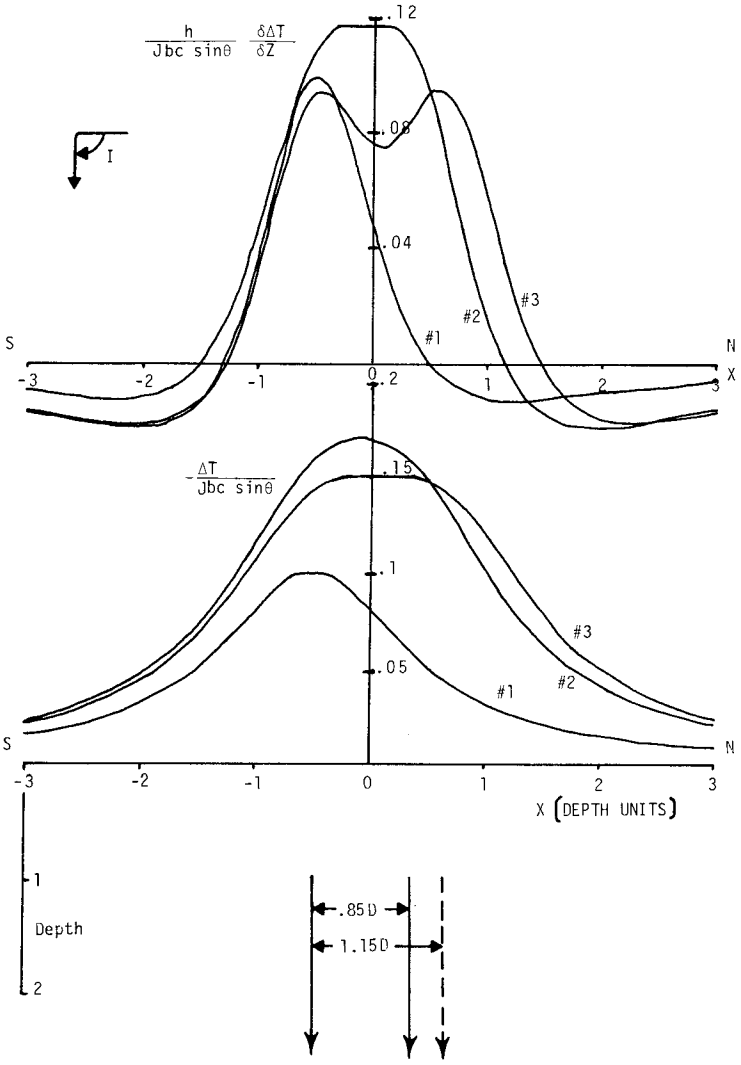

Figure 7.26. *Normalized theoretical total field and vertical gradient profiles due to:*

#1 - a single thin vertical dyke;

#2 - two thin dykes whose separation is 0.85 times their depth of burial — the limit of resolution for the total field anomalies;

#3 - two thin dykes whose separation is 1.15 times their depth of burial — the limit of separation for the vertical gradient anomalies.

Inclination of the earth's field is 90°.

AEROMAGNETIC GRADIOMETER SURVEYS

The vertical gradiometer has many advantages over the single sensor instrument. The first advantage is that the gradiometer records essentially only the magnetic field produced by the rock formations in the upper part of the earth's crust. This is, of course, the required signal and the noise (see Fig. 7.25) which consists of a time-varying component that is the effect of diurnal variation is automatically removed, together with the main earth's field produced by the earth's core and most of the long-wavelength anomalies due to deep-seated bodies in the crust.

However, the most impressive feature is the greatly improved resolution of the gradiometer compared to the total field instrument due to the fact that vertical gradient anomalies are always narrower than their associated total field anomalies. This fact is illustrated in Figure 7.26 which shows the theoretical total field (ΔT) and vertical gradient ($\frac{\partial \Delta T}{\partial Z}$) anomalies due to a thin vertical dyke model where the dip of the earth's field is 90°. The ordinate values have been normalized for amplitude and the abscissal values are expressed in depth units. The nomenclature used is that of Hood (1971) where D is the half-width to depth ratio.

Anomaly 1 is the anomaly produced by a single thin vertical dyke and it can be seen that the vertical gradient anomaly is much narrower than the total field anomaly. Anomalies 2 and 3 are for two thin dykes whose distance apart is at the limit of resolution of the combined total field and vertical gradient anomalies respectively. The limit of resolution is here defined as being the maximum separation of the dykes where the top of the anomaly is still flat without breaking downward at the top to show that two anomalies are present. For the total field case, the separation has to be at least 1.15 D for the two dykes to be resolved but only 0.85 D in the case of vertical gradient measurements. Thus vertical gradient measurements have a 30 per cent better resolving capability for the thin dyke case at high magnetic latitudes than for total field measurements.

The superior resolution of vertical gradient data is, of course, also readily apparent from a comparison of actual total field and vertical gradient profiles. Figure 7.27 shows such a comparison from the survey flown in the Kasmere Lake area of Manitoba (GSC Open File 528, 1978). The anomalous zone on the left hand end of the profile can from the vertical gradient profile be seen to consist of at least 9 recognizable anomalies which have been labelled from A to I in both the total field and vertical gradient profiles. For comparison purposes amplitudes of the anomalies have been normalized with respect to anomaly F. Two anomalies, J and K, occur on the flank of the anomalous zone and L is an isolated anomaly. It can be seen that composite anomalies CD, EFG and HI are below the resolution of the total field instrument whereas for the vertical gradiometer each of the anomalies has been clearly resolved from its neighbour. Note also that the relative amplitudes of the vertical gradient anomalies differ from the total field ones (although this comparison is complicated by the interference of adjacent anomalies except for the case of anomaly L). However vertical gradient anomaly H has clearly been amplified in comparison with anomalies B or C, and this is due to the shorter wavelength of anomaly H. The shorter wavelength features will in general be produced by near-surface causative bodies, so the vertical gradiometer tends to emphasize the magnetic effects of the near-surface geology over deep-seated features. Thus it is a better geological mapping tool than the single sensor instrument.

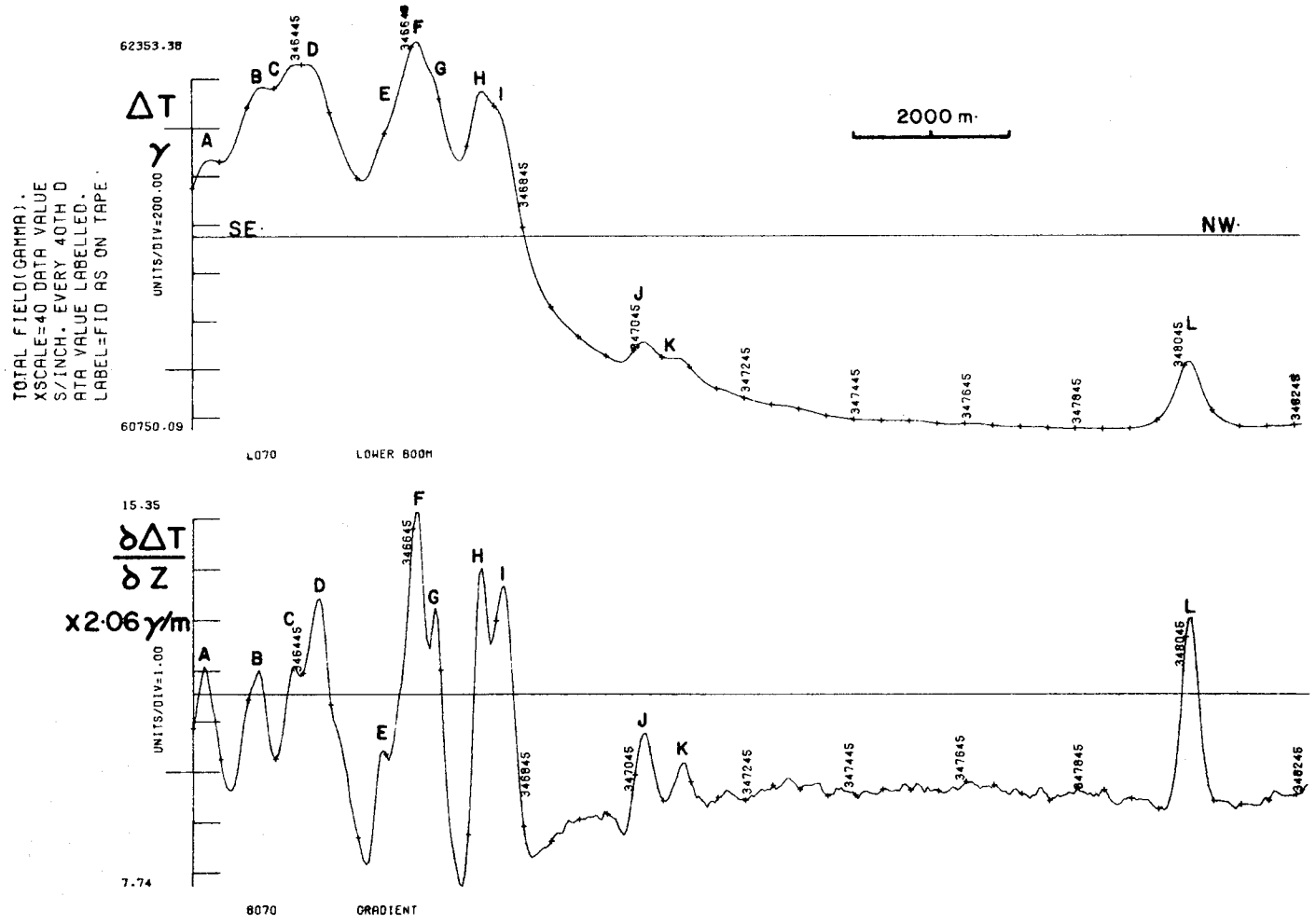

Figure 7.27. *Aeromagnetic profiles demonstrating the superior resolution of vertical gradient over total field data, Kasmere Lake, Manitoba (GSC Open File 528, 1978).*

In Figures 25.2 and 25.3 of Paper 25 of this volume, Coope and Davidson (1979) have presented the vertical gradient and total field maps of a survey flown over the White Lake granite pluton in southeastern Ontario. Figure 25.1 in the same paper is part of GSC geological map 1046A (Quinn, 1952) covering the survey area. The airborne results were also issued as Open File Report 339 by the Geological Survey of Canada (Hood et al., 1976). It is readily apparent from a comparison of the maps that a greater amount of geological information of a more precise nature may be derived from vertical gradient maps. For instance, the two diabase dykes that cut the granite pluton are much narrower on the vertical gradient map. It should be noted in those maps that there is evidence of zoning within the granite pluton itself in the vertical gradient map and several fault zones are evident. In fact, fault zones are much more readily apparent on vertical gradient than on total field maps. Thus vertical gradient aeromagnetic surveys would appear to be of particular value in porphyry copper exploration programs. It should however be pointed out that a somewhat closer flight line spacing must be used in aeromagnetic gradiometer surveys because of the higher resolution of the technique in order to avoid coherency problems. We conclude that vertical gradient aeromagnetic surveys are a viable alternative to total or vertical field ground magnetic surveys.

Another important property of vertical gradient data is its ability to delineate geological contacts because Precambrian Shield areas usually consist of rock formations of relatively large areal extent separated from one another by steeply dipping contacts. Figure 7.28 shows the resultant vertical gradient (solid line) and total field (dashed line) curves over a wide elongated rock formation with sloping sides which is located at a high magnetic latitude such as Canada. For this particular geometric model, actually a dyke, the half width to depth ratio is 5. For comparison purposes, the amplitude of the two curves has been made approximately equal. It can be seen that there are two cross-overs from positive to negative values for the vertical gradient profile with the zero gradient values occurring close to either of the contacts. In contrast, the total field anomaly is much less definitive in delineating the edges of the causative rock formation. Actually if the dip of the earth's field and the contacts were vertical, then the zero gradient value would accurately coincide with the position of the contact. However, it can be shown mathematically that the line joining the maximum and minimum gradient values crosses the vertical gradient profile itself at the point where the contact is located. This important property has been illustrated in Figure 7.28. Thus on vertical gradient aeromagnetic maps flown at high magnetic latitudes, the zero gradient contours will delineate the contacts of major rock formations having some measurable magnetization contrast with adjacent formations in a reasonably accurate fashion.

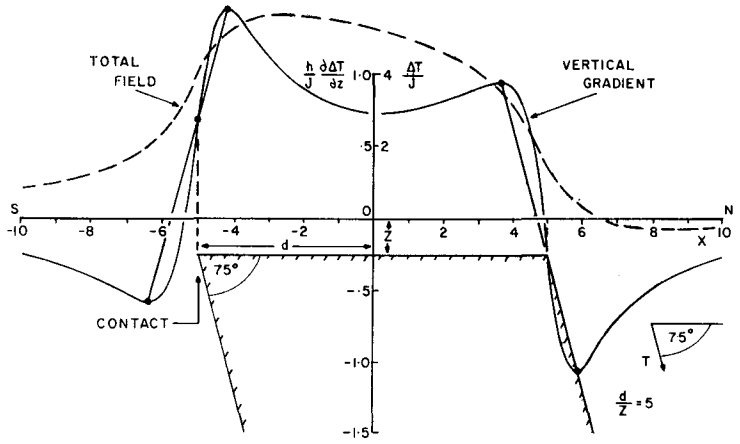

Figure 7.28. *Vertical gradient and total field profiles over a wide dipping dyke; inclination of the earth's magnetic field = 75°.*

It follows therefore that vertical gradient aeromagnetic survey results are in fact a better tool for geological mapping programs than the more conventional total field results. Moreover, because many orebodies are located at or near contacts, the vertical gradient technique should prove invaluable in tracing such contacts using airborne techniques.

There is a great deal of aeromagnetic survey data available throughout the world and it is possible to derive the first vertical gradient data from the total field results. Although there is some loss of accuracy when compared with the measured vertical gradient data (Hood et al., 1976), nevertheless the resultant end product reflects the underlying geology much better than the total field map. McGrath et al. (1976) has devised a compilation procedure for the purpose which uses a two-dimensional vertical gradient operator (McGrath, 1975). It is necessary, however, that the total field data be of high quality without significant levelling errors because these tend to be emphasized in the resultant map.

Thus to summarize, the main advantages of the aeromagnetic gradiometer as a geological mapping tool compared to the single sensor (total field) technique are:

- direct delineation of vertical contacts by the zero gradient contour value, i.e. vertical contact mapper;
- superior resolution of anomalies produced by closely-spaced geological formations;
- anomalies produced by near-surface features are emphasized with respect to those resulting from more deeply-buried rock formations; and
- regional gradient of the earth's magnetic field and diurnal variation are automatically removed.

REGIONAL MAGNETIC ANOMALY MAPS

Recognition of the value of regional magnetic compilations has grown appreciably in the last decade since the first magnetic anomaly map of Canada, and probably the first such map of its kind in the world, was presented at the 1967 symposium in Niagara Falls by Morley et al. (1968). A third edition of the Magnetic Anomaly Map of Canada was published by the Geological Survey of Canada (McGrath et al., 1977) in time for the Exploration 77 Symposium. The map was derived from approximately 8250 1:63 360 total-field aeromagnetic maps and was published at the scale of 1:5 000 000 using a colour contour interval of 200 γ. Sea magnetometer data were also included. For the compilation, the main geomagnetic field which has its origin in the earth's core was subtracted from the map data by a graphical separation technique (McGrath et al., 1978). Thus the residual magnetic features shown in this map are related mainly to sources within the crust of the earth. Because of the small scale of the map, magnetic features less than 8 km wide do not show up. Hence the map can be regarded as reflecting large-scale near-surface and major deep-seated crustal features. The main uses of a map of this type are threefold. Firstly, as an index map it presents an overview of the aeromagnetic survey coverage of Canada. Secondly, the map presents the major patterns produced by the continental rocks in the Canadian landmass and may be used both as an aid in the interpretation of regional geological features in the basement rocks as well as to help in the planning of more detailed investigations. Lastly and probably the most important use of the map is as a vehicle or medium to initially stimulate comparisons of magnetic features with other types of geoscientific compilations.

Plate 1 shows part of the area extending from James Bay on the east to the Province of Manitoba on the west from the Magnetic Anomaly Map of Canada. The large magnetic high areas (red) correlate well with terrain underlain by rocks of granitic composition. Also there is an obvious correspondence between greenstone belts and their metamorphic equivalents with the broad magnetic low areas (green). For example, the Wabigoon volcanic belt (WB) is associated with a magnetic low. Thus it is within the broad magnetic low areas in which most of the economic ore deposits occur. Locally magnetic highs in greenstone belts are associated with iron formation, iron-rich tholeiitic basalts and iron-rich basic intrusive rocks. Volcanic rocks of calc-alkaline and komatiitic affinities are generally nonmagnetic.

The continuity of the magnetic patterns over large areas is particularly evident and contrast with the variation in the patterns from one area to another. Some of the magnetic anomaly pattern changes occur at geological province boundaries. For example, the trace of the change from the predominantly east-west trending anomalies in the magnetic high area over northwestern Ontario as compared to the magnetic low northeast-southwest trends to the northwest in Manitoba delineates the edge of the Churchill-Superior province (CSB).

Other pattern changes occur within a given geological province. The Kapuskasing Lineament (KL) extending from James Bay to the eastern end of Lake Superior is a structural zone within a geological province in which both the magnetic base level and the magnetic anomaly patterns change. On the other hand, the Quetico structural zone (QS) is associated with a linear magnetic low which transgresses through the magnetic anomaly pattern associated with the western Superior province.

It seems apparent from the examples presented in the foregoing discussion that in general a great deal of correlation exists between the magnetic and geologic compilations and that the production of such national magnetic anomaly maps is worthwhile and should be encouraged by other nations.

A number of interesting regional magnetic studies have been carried out by workers in various countries and among the more interesting are those by McGrath and Hall, 1969; Hall and Dagley, 1970; Kornik, 1971; Zietz et al., 1971; Krutikhovskaya et al., 1973; Hood and Tyl, 1977.

International Geomagnetic Reference Field

As aeromagnetic coverage of large continental areas was completed during the early sixties and the results were

compiled into regional magnetic anomaly maps, the need to eliminate the dominating effect of the earth's main field became apparent. In a country such as Canada the earth's magnetic field varies by an amount of 7000 γ or so in going from the east and west coasts to the centre of the country. The amplitude of anomalies due to crustal rocks except in the case of magnetic iron formation is less than 1000 γ. Consequently if the main field which is due to the magnetic properties of the earth's core were not removed, the resultant map would be dominated by a series of parallel contours due to the main earth's field and there is a consequent distortion of the crustal anomalies e.g. the peaks are displaced. If the main earth's field is removed, it is possible to produce a coloured map utilizing four or five colours each representing a 200 γ contour interval to represent the crustal magnetic field. Accordingly a mathematical model of the main earth's field called the International Geomagnetic Reference Field (IGRF 1965.0) was adopted at the Symposium on the Description of the Earth's Magnetic Field held in Washington from October 22-25, 1968. The 1965.0 IGRF was defined by a set of spherical harmonic coefficients to degree and order 8, which requires 80 coefficients, and a linear secular variation correction was incorporated (Fabiano and Peddie, 1969; Cain and Cain, 1971). It has transpired that the secular variation corrections chosen were not particularly accurate and this has resulted in errors of the IGRF of up to a few hundred gammas in five years (Regan and Cain, 1975). At the Grenoble Assembly of the IUGG in 1975 it was resolved that IGRF 1965.0 be replaced by IGRF 1975.0 to be used until at least 1980. This new model consists of IGRF 1965.0 brought up to epoch 1975.0 for its main field coefficients plus new coefficients for secular change (Barraclough and Fabiano, 1977). It is hoped that with the launching of U.S. magnetic field satellite (Magsat) in September 1979, that an analysis of the resultant data will result in a more accurate mathematical model of the earth's magnetic field (Cain, 1971; Langel et al., 1977).

SUMMARY AND CONCLUSIONS

During the past decade both ground and airborne magnetometers have been improved considerably by miniaturization and made more reliable by the extensive use of integrated circuit devices. Digital-recording of aeromagnetic survey data is now standard procedure and except for the flight recovery process, the compilation of aeromagnetic maps is now a completely automated process. The resultant gridded data generated for the machine contouring process also facilitate the production of a variety of derived and processed maps to any scale or map projection for use in the subsequent interpretation of the aeromagnetic data. Aeromagnetic gradiometry has also been proven to be a useful tool in the mapping of Precambrian terrane.

Quantitative interpretation methods have seen noticeable advances during the past decade particularly those using the computer to match observed and calculated anomalies by a best-fit process.

Thus after more than a quarter century the aeromagnetic survey technique is still being improved in many new and novel ways and it remains the most utilized airborne survey technique in terms of the line kilometrage flown each year throughout the world. This continued popularity is due in part to a variety of reasons. Of all the airborne geophysical survey techniques, the aeromagnetic method has by far the greatest depth penetration being able to detect features down to the Curie point geotherm some 20 km or so beneath the earth's surface. Moreover in contrast to other airborne techniques, the aeromagnetic method is unaffected by the presence of surficial material such as overburden and tropical weathering or by the presence of lakes and swamps. Aeromagnetic surveys also provide a continuity of information at low cost that is impossible to achieve in ground geophysical or geological surveys, and one of the outstanding advantages of aeromagnetic surveys becomes apparent when large areas are surveyed because large regional geological features are often discovered. These may not be recognizable on the ground because they are so large or are perhaps obscured by sedimentary formations. Clearly further significant developments in the aeromagnetic survey technique can be expected in the next decade especially in the application of digital recording and processing techniques.

REFERENCES

Am, K.
1972: The arbitrarily magnetized dyke: interpretation by characteristics; Geophys. Explor., v. 10 (2), p. 63-90.

Andreasen, G.E. and Zietz, I.
1969: Magnetic fields for a 4 x 6 prismatic model; U.S. Geol. Surv., Prof. Paper 666, 219 p.

Barraclough, D.R. and Fabiano, E.B.
1977: Grid values and charts for the IGRF 1975.0; Int. Assoc. Geomag. Aeron., Bull. 38, 134 p.

Bott, M.H.P. and Hutton, M.A.
1970: A matrix method for interpreting oceanic magnetic anomalies; Geophys. J. v. 20 (2), p. 149 157.

Cain, J.C.
1971: Geomagnetic models from satellite surveys; Rev. Geophys. Space Phys., v. 9, p. 259-273.

Cain, J.C. and Cain, S.J.
1971: Derivation of the International Geomagnetic Reference Field; NASA, Tech. Note D-6237 (IGRF 10/68).

Collin, C.R., Salvi, A., Lemercier, D., Lemercier, P., and Robach, F.
1973: Magnétomètre différentiel à haute sensibilité; Geophys. Prosp., v. 21 (4), p. 704-715.

Coope, J.A. and Davidson, M.J.
1979: Some aspects of integrated exploration; in Geophysics and Geochemistry in the Search for Metallic Ores, Geol. Surv. Can., Econ. Geol. Rep. 31, Paper 25.

Dutton, D.H. and Nisen, W.G.
1978: The expanding realm of computer cartography; Datamation, p. 134-142, June 1978.

Fabiano, E.B. and Peddie, N.W.
1969: Grid values of total magnetic intensity IGRF-1965; U.S. Env. Sci. Serv. Admin., Tech. Rept. 38, 55 p.

Geological Survey of Canada
1978: Aeromagnetic gradiometer survey, Kasmere Lake area, Manitoba; Geol. Surv. Can., Open File 528.

Goree, W.S. and Fuller, M.
1976: Magnetometers using RF-driven Squids and their applications in rock magnetism and paleomagnetism; Rev. Geophys. Space Phys., v. 14 (4), p. 591-608.

Grant, F.S.
1972: Review of data processing and interpretation methods in gravity and magnetics, 1964-1971; Geophysics, v. 37 (4), p. 647-661.

1974: Timmins magnetic susceptibility map; Geol. Surv. Can., Open File 229.

Hahn, A.
1978: Die Einheiten des internationalen Systems in der Geomagnetik; J. Geophys., v. 44, p. 189-202.

Hall, D.H. and Dagley, P.
1970: Regional magnetic anomalies: an analysis of the smoothed aeromagnetic map of Great Britain and Northern Ireland; Inst. Geol. Sci., UK, Rep. 70/10, 8 p.

Hartman, R.R., Teskey, D.J., and Friedberg, J.L.
1971: A system for rapid digital aeromagnetic interpretation; Geophys., v. 36 (5), p. 891-918.

Holroyd, M.T.
1974: The aeromagnetic data automatic mapping (ADAM) system; in Report of Activities, Part B, Geol. Surv. Can., Paper 74-1B, p. 79-82.

Holroyd, M.T. and Bhattacharyya, B.K.
1970: Automatic contouring of geophysical data using bicubic spline interpolation; Geol. Surv. Can., Paper 70-55, 40 p.

Hood, P.
1970: Magnetic surveying instrumentation; a review of recent advances; in Mining and Groundwater Geophysics 1967 (L.W. Morley, Ed.), Geol. Surv. Can., Econ. Geol. Rep. 26, p. 3-31.

1971: Geophysical applications of high resolution magnetometers; in Encyclopedia of Physics, Springer-Verlag, Berlin, v. 49 (3), p. 422-460.

1972: Mineral exploration: trends and developments in 1972; Can. Min. J., v. 93 (2), p. 175-199.

1973: Mineral exploration: trends and developments in 1972; Can. Min. J., v. 94 (2), p. 167-182.

1976: Mineral exploration: trends and developments in 1975; Can. Min. J., v. 97 (2), p. 163-197.

1977: Mineral exploration: trends and developments in 1976; Can. Min. J., v. 98 (1), p. 8-47.

1978: Mineral exploration: trends and developments in 1977; Can. Min. J., v. 99 (1), p. 8-53.

Hood, P., Sawatzky, P., Kornik, L.J., and McGrath, P.H.
1976: Aeromagnetic gradiometer survey, White Lake, Ontario; Geol. Surv. Can., Open File 339.

Hood, P. and Tyl, I.
1977: Residual magnetic anomaly map of Guyana and its regional geological interpretation; Mem. Second Latin Amer. Cong., Caracas, v. 3, p. 2219-2235.

Hood, P. and Ward, S.H.
1969: Airborne geophysical methods; in Advances in Geophysics, Academic Press, New York, v. 13, p. 1-112.

IAGA
1973: Adoption of SI units in geomagnetism; Trans. 2nd Gen. Sci. Assembly, Int. Assoc. Geomag. Aeronomy, Kyoto, Japan, 1973, Bull. 35, p. 148 151.

Johnson, W.W.
1969: A least-squares method of interpreting magnetic anomalies caused by two-dimensional structures; Geophysics, v. 34 (1), p. 65-74.

Kornik, L.J.
1971: Magnetic subdivision of Precambrian rocks in Manitoba; Geol. Assoc. Can., Spec. Paper 9, p. 51 60.

Koulomzine, T., Lamontagne, Y., and Nadeau, A.
1970: New methods for the direct interpretation of magnetic anomalies caused by inclined dikes of infinite length; Geophysics, v. 35 (5), p. 812-830.

Krutikhovskaya, Z.A., Pashkevich, I.K., and Simonenko, T.N.
1973: Magnetic anomalies of Precambrian Shields and some problems of their geological interpretation; Can. J. Earth Sci., v. 10 (5), p. 629-636.

Langel, R.A., Regan, R.D., and Murphy, J.P.
1977: Magsat: a satellite for measuring near earth magnetic fields; Goddard Space Flight Center, Rep. X-922-77-199.

Lantto, V.
1973: Characteristic curves for interpretation of highly magnetic anomalies in borehole measurements; Geoexpl., v. 11 (2), p. 75-85.

McGrath, P.H.
1975: A two-dimensional first vertical derivative operator; in Report of Activities, Part A, Geol. Surv. Can., Paper 75-1A, p. 107-108.

McGrath, P.H., Haley, E.L., Reveler, D.A., and Letourneau, C.P.
1978: Compilation techniques employed in constructing the Magnetic Anomaly Map of Canada; in Current Research, Part A, Geol. Surv. Can., Paper 78-1A, p. 509-515.

McGrath, P.H. and Hall, D.H.
1969: Crustal structure in northwestern Ontario: regional magnetic anomalies; Can. J. Earth Sci., v. 6 (1), p. 101-107.

McGrath, P.H. and Hood, P.J.
1970: The dipping dike case: a computer curve-matching method of magnetic interpretation; Geophysics, v. 35 (5), p. 831-848.

1973: An automatic least-squares multi-model method for magnetic interpretation; Geophysics, v. 38 (2), p. 349-358.

McGrath, P.H., Hood, P.J., and Darnley, A.G.
1977: Magnetic anomaly map of Canada; Geol. Surv. Can., Map 1255A (3rd Ed.).

McGrath, P.H., Kornik, L.J., and Dods, S.D.
1976: A method for the compilation of high quality calculated first vertical derivative aeromagnetic maps; in Report of Activities, Part C, Geol. Surv. Can., Paper 76-1C, p. 9-17.

Morley, L.W., MacLaren, A.S., and Charbonneau, B.W.
1968: Magnetic anomaly map of Canada; Geol. Surv. Can., Map 1255A (1st Ed.).

Naudy, H.
1971: Automatic determination of depth on aeromagnetic profiles; Geophysics, v. 36 (4), p. 717-722.

O'Brien, D.P.
1970: Two-dimensional inverse convolution filters for analysis of magnetic field; 40th Ann. Int. Meet., Soc. Explor. Geophys., New Orleans (Abstr.).

1971: An automated method for magnetic anomaly resolution and depth-to-source computation; Proc. Symp. on Treatment and Interpretation of Aeromagnetic Data, Berkeley, California.

1972: Compudepth: a new method for depth-to-basement computation; 42nd Ann. Mtg., Soc. Explor. Geophys., Anaheim, California (Preprint).

Ogawa, K. and Tsu, H.
1976: Magnetic interpretation using interactive computer graphics; Japan Pet. Dev. Corp., Tech. Res. Center, Rep. 3, p. 19-39.

Otala, M.
1969: The theory and construction of a proposed superconducting aeromagnetic gradiometer; Acta Polytech. Scand., Helsinki, Elect. Eng. Ser. 21, 55 p.

Quinn, H.A.
1952: Renfrew map area, Renfrew and Lanark Counties, Ontario; Geol. Surv. Can., Paper 51-27, 79 p.

Rao, B.S.R., Murthy, I.V.R., and Rao, C.V.
1973: Two methods for computer interpretation of magnetic anomalies of dikes; Geophysics, v. 38 (4), p. 710-718.

Regan, R.D. and Cain, J.C.
1975: The use of geomagnetic field models in magnetic surveys; Geophysics, v. 40 (4), p. 621-629.

Sarwinski, R.E.
1977: Superconducting instruments; Cryogenics, p. 671 679, Dec.

Sawatzky, P. and Hood, P.J.
1975: Fabrication of an inboard digital-recording vertical gradiometer system for aeromagnetic surveying: a progress report; in Report of Activities, Part A, Geol. Surv. Can., Paper 75-1A, p. 139-140.

Spector, A. and Grant, F.S.
1970: Statistical models for interpreting aeromagnetic data; Geophysics, v. 35 (2), p. 293-302.

Spector, A. and Parker, W.
1979: Computer compilation and interpretation of geophysical data; in Geophysics and Geochemistry in the Search for Metallic Ores, Geol. Surv. Can., Econ. Geol. Rep. 31, Paper 23.

Steenland, N.C.
1970: Recent developments in aeromagnetic methods; Geoexplor., v. 8 (3/4), p. 185-204.

Zablocki, C.J.
1974: Magnetite assays from magnetic susceptibility measurements in taconite production blast holes; Geophysics, v. 39 (2), p. 174-189.

Zietz, I., Hearn, B.C., Higgins, M.W., Robinson, G.D., and Swanson, D.A.
1971: Interpretation of an aeromagnetic strip across the northwestern United States; Geol. Soc. Am. Bull., v. 82 (12), p. 3347-3372.